β-Fluorinated Paraconic Acid Derivatives: Synthesis and Fluorine Stereoelectronic Effects

Fioretta Asaro [a], Sara Drioli [a], Paolo Martinuzzi [b], Patrizia Nitti [a,*], Daniele Toffoli [a], Sofia Zago [a], Daniele Zuccaccia [b]

[a] Department of Chemical and Pharmaceutical Sciences, University of Trieste, via Licio Giorgieri 1, 34127 Trieste, Italy
[b] Department of Agricultural, Food, Environmental and Animal Sciences DI4A, University of Udine, Via Cotonificio 108, 33100 Udine, Italy

ARTICLE INFO

Keywords:
Selectfluor®
lactones
butenolides
^{19}F NMR
DFT
RDkit

ABSTRACT

New methods for the introduction of fluoro substituents are in great demand, owing to the present importance of fluorinated bioactive compounds. Here we report a simple strategy for the synthesis of a new class of β-fluorinated paraconic acid derivatives. Methyl and ethyl hexanoyl succinates were fluorinated by Selectfluor®, then reduced by a mild reducing agent in acidic medium, thus partially suppressing the HF elimination reaction. The diastereomeric β-fluoro-γ-lactones afforded by lactonization of the fluorinated hydroxydiesters were separated by column chromatography. Their stereochemistry was assessed by means of ^{19}F{^{1}H}-HOESY NMR measurements. The relationship between the remarkable ^{19}F chemical shift difference (20 ppm) and configuration difference was elucidated by two-component relativistic DFT calculations. Both the quick survey of conformers stability based on molecular mechanics in the RDKit environment and the DFT geometry optimizations at the scalar ZORA TZ2P/BLYP level, revealed that for the (2*R*,3*R*) diastereomer the γ-lactone ring adopts one prevalent envelope conformation, whereas for the (2*R*,3*S*) one both envelope conformations must be taken into consideration.

1. Introduction

The presence of a fluorine atom characterizes pharmaceutical compounds with very different activities that are steadily gaining momentum in the pharmaceutical market [1-4]. The introduction of fluorine may exert benign effects on both therapeutic properties and metabolic stability [5,6]. A strategy in the quest for new drugs is the modification of natural products [7] and the introduction of fluorine, element uncommon in natural organic compounds, is an interesting opportunity [8]. The development of new fluorinated molecules is boosted by the modern fluorination methods, much easier and safer than previous ones [9].

Paraconic acids are an important class of natural, highly functionalized, γ-lactones bearing, as characteristic functionality, a carboxylic acid group at C-β [10–12]. Due to their wide spectrum of biological activities, including antitumor, antibiotic, antifungal, and antibacterial effects, the synthesis of paraconic acids and their derivatives is of continuing interest [13-16].

Site selective fluorination of paraconic acids by Selectfluor® has been reported, which affords β-fluorinated γ-lactones, in which the carboxylic moiety has gone lost due to concomitant decarboxylation [17]. We decided to investigate the synthesis of a new class of fluorinated γ-alkyl paraconic acids, which keep the carboxylic functionality, and therefore we used an alternative strategy with respect to direct fluorination of the γ-lactone ring. Considering that the easiest route for the achievement of γ-alkylparaconic acids consists in a reduction-lactonization sequence of acylsuccinates [18-21] and that β-ketoesters can be easily fluorinated by Selectfluor® [22-24] we chose acylsuccinates as the precursors. Specifically, we report here the synthesis of fluorinated lactones **6a,b** and **7a,b** (Scheme 1) exploiting **1a,b** hexanoylsuccinates precursors, which in previous works were easily converted into methylenolactocin [25,26]. In addition, we could synthesize by the same route the simplest analogues bearing a methyl group in place of the pentyl chain, the fluorinated lactones **10** and **11** (Scheme 4).

The problem of the assignment of the relative stereochemistry of the obtained fluorinated γ-lactones can in general be solved by X-ray diffraction crystallography [27], or from NOESY experiments [17] and by analysis of NMR spectra [28]. A recognized and widely exploited tool in structural studies by NMR, owing to the remarkable angular

* Corresponding author. Phone number: +39 040 5583923
E-mail address: pnitti@units.it (P. Nitti).

Accepted 25 July 2021

dependence, are vicinal coupling constants, especially the proton proton ones, ^{3}J(H,H) [29], but also the ^{3}J(H,F) [30]. However, in the case of flexible molecules they do not provide immediate information because they are the result of the averaging over different conformations. Relevant examples are variously substituted γ-butyrolactones, where the assessment of stereochemistry by means of ^{3}J(H,H) required a previous conformational analysis [31-33], and analogous considerations apply for the present fluorinated γ-butyrolactones. Here, we exploited NMR methods, profiting of the presence of the ^{19}F nucleus [3], especially through the information provided by ^{19}F{^{1}H}-HOESY experiments [34] and by ^{19}F chemical shift computational calculations.

2. Result and discussion

2.1. Synthesis of Fluorinated Paraconic Acid Derivatives

Dimethyl and diethyl hexanoylsuccinates **1a,b** were prepared by radical addition of hexanal to dimethyl or diethyl maleate [35,36], Aiming at synthesizing β-fluorinated methylenolactocin, which bears a pentyl chain in γ-position, we selected hexanal as starting material. The following fluorination reaction with Selectfluor® was optimized on methyl ester **1a**, both by conventional heating (75-80°C in CH_3CN/H_2O, ratio 4:1 v/v, 46 h, 85% yield) and by microwave irradiation (MW) [23] (78°C in CH_3CN/H_2O, ratio 4:1 v/v, 4 h, 44% yield, Scheme 2).

Fluorinated ketodiester **2a** was firstly reduced with $NaBH_4$. The use of 2 eq of $NaBH_4$ led to a complex mixture of defluorinated compounds, elimination of fluoride ion under basic conditions being a common problem [37]. However, using 0.5 eq of $NaBH_4$, hydroxydiester **3a** and lactone **5a** (5:2 ratio) were the main products. There wasn't any evidence in the NMR spectra of the crude reaction mixture of the presence of **4a** and the separation of these compounds by flash chromatography led to the isolation of **3a** (^{19}F NMR -171.6 ppm, 25% yield), **5a** (9% yield) beside a small amount of the enol-γ-lactone **8a** [38], deriving from double bond isomerization of **5a**. The treatment with trifluoroacetic acid (TFA) of purified **3a** afforded lactone **6a** (^{19}F NMR -152.75 ppm, dt, J = 26.6, 21.8 Hz) in almost quantitative yield, as a single diastereomer (Scheme 3).

The low yield of desired product **3a** induced us to try other reduction methods. Attempts of ketodiester **2a** hydrogenation catalyzed by Pd or Pt on carbon failed. On the contrary, the reduction of **2a** with $NaBH_3CN$ under acidic conditions was successful leading to a mixture of hydroxydiesters **3a** (^{19}F NMR -171.6 ppm) and **4a** (^{19}F NMR -175.2 ppm), in about 3:1 ratio, and butenolide **5a** as a minor product. The same reduction carried out on **2b** afforded **3b** (^{19}F NMR -171.5 ppm) and **4b** (^{19}F NMR -175.1 ppm), in about 3:2 ratio, and traces of lactone **5b** [39] (Scheme 3). Acidic lactonisation of the mixture of hydroxydiesters **3a** and **4a** led to formation of lactones **6a** (^{19}F NMR -152.75 ppm, dt, J = 26.6, 21.8 Hz, 67% yield) and **7a** (^{19}F NMR -173.66 ppm, dt, J = 34.9, 21.3 Hz, 11% yield). Analogously, lactonic esters **6b** (-152.59 ppm, dt, J = 26.5, 21.8 Hz, 43% yield) and **7b** (^{19}F NMR δ -173.71 ppm, dt, J = 34.7, 21.3 Hz, 19% yield) were isolated from acidic lactonisation of the mixture of **3b** and **4b**. To avoid decomposition of fluorinated products, diastereomeric lactones **6** and **7** had to be separated by flash chromatography only after acidic treatment of silica gel (Scheme 3).

To prove that the large difference in the chemical shift of the fluorine of the two diastereomeric lactones **6** and **7** was independent of the γ-alkyl chain length, the same reactions were carried out using dimethyl acetylsuccinate, commercially available starting material (Scheme 4). From fluorinated ketodiester **9**, lactones **10** (**10** ^{19}F NMR δ -153.17 ppm, dt, J = 28.4, 21.7 Hz), **11** (**11** ^{19}F NMR δ -173.7 ppm, dtq, J = 34.9, 22.4, 2.6 Hz) and **12** in the respective 2:1:2.6 ratio were obtained. After purification by flash chromatography an inseparable mixture of lactones **10** and **12** in the respective 2:3 ratio (about 40% yield) and lactone **11** (10% yield) were recovered.

2.2. NMR characterization of Stereochemistry

To determine the stereochemistry of fluorinated γ-lactones, the ^{19}F{^{1}H}-HOESY NMR spectra of lactones **6b** and **7b** were recorded and carefully analyzed. Concerning lactone **6b**, strong correlations are present between the F and H-2 and H-4 (at 2.93 ppm). (Figure 1a). Medium-low strength NOE cross-peak is observed between F and H-4 (at 3.36 ppm). Very low-strength correlations are observed between F and H-1' of the first methylene of the pentyl chain, whereas F does not show any interaction with the hydrogens of ester ethyl chain. This NOE pattern indicates that F is in the opposite side of the pentyl chain, near H-4 *cis* (that resonates at 2.93 ppm) and H-2 and far away from H-4 *trans* (at 3.36 ppm). With this pattern of NOE signal in hand, it is clear that the stereochemistry of fluorinated γ-lactone **6b** is *rel*-(2*R*,3*S*). A quantitative analysis of the heteronuclear NOE intensities was carried out taking into account that the volumes of the cross peaks are proportional to ($n_H n_F$/n_H+n_F), where n_H and n_F are the number of equivalent H and F nuclei, respectively (Table S1) [40,41].

Average F-H distances in solution were derived from the NOE measurements taking the distance between F and H-2 (2.5 Å) as reference (Table S1) [40,42]: the value of 2.5 Å is obtained from the most stable conformation, see below DFT geometry optimization. In addition, it was assumed that all protons have a slow local correlation time [43,44], see SI for details. It is well known that the structure of flexible molecules is much more difficult to be determined (this is beyond the scope of this paper) compared to rigid molecules, and only averaged NMR parameters are accessible in a qualitative manner. [45] The average distances between F and H-4 *trans*, H-4 *cis*, and hydrogens H-1' obtained from ^{19}F{^{1}H}-HOESY experiments are 3.0, 2.4 and 3.6 Å, respectively. The distances compare well with those from DFT calculation (Table S2). Concerning lactone **7b**, a strong NOE cross-peak is present between the F and H-4 *cis* (at 3.25 ppm) (Figure 1b). Medium strength correlations are observed between F and H-2, H-4 *trans* (at 2.96 ppm) and hydrogens H-1' of the first methylene of the pentyl chain, whereas F does not show any interaction with the ester ethyl chain. This NOE pattern indicates that F is located near the pentyl chain in the opposite side of H-2. With this pattern of NOE signal in hand, it is clear that the stereochemistry of fluorinated γ-lactone **7b** is *rel*-(2*R*,3*R*). As previously described, the average distances between F and protons H-2 and H-4 *trans* obtained from ^{19}F{^{1}H}-HOESY experiments (taking the distance between F and H-4 *cis* atoms equal to 2.5 Å, obtained from the most stable conformation, as reference, see below DFT geometry optimization) are both 3.1 Å, in good agreement with DFT results (Table S2), and the average distance between F and H-1' protons is 3.3 Å.

2.3. Preliminary Molecular Mechanics conformational search and DFT geometry optimization

The observed sizeable chemical shift difference of fluorine looks promising as a quick and easy method to differentiate the diastereomers of the substituted butyrolactone. Theoretical calculations were carried out aiming at understanding its origin.

Owing to the high flexibility of the molecules and the consequent high number of possible conformers, a preliminary screening was performed by generating 100 conformers for one enantiomer of each diastereomer of the methyl esters, specifically for the (2*R*,3*S*)-**6a** and (2*R*,3*R*)-**7a**, where the carboxylic group and pentyl chain substituents are *cis* and *trans*, respectively. The same procedure was followed for the ethyl esters (2*R*,3*S*)-**6b** and (2*R*,3*R*)-**7b**.

The most important degrees of freedom are those related to the ring puckering, with the C-3 atom lying, either above the average plane passing through the remaining ring atoms, conformation ^{3}E, or below in conformation E_3. We introduce the terms F pseudo-axial and F pseudo-equatorial [46] to address the conformation pairs in the racemic mixture that are equivalent under the respect of non chiral properties. Thus, with F pseudo-axial conformation for **6** we mean any member of the mirror

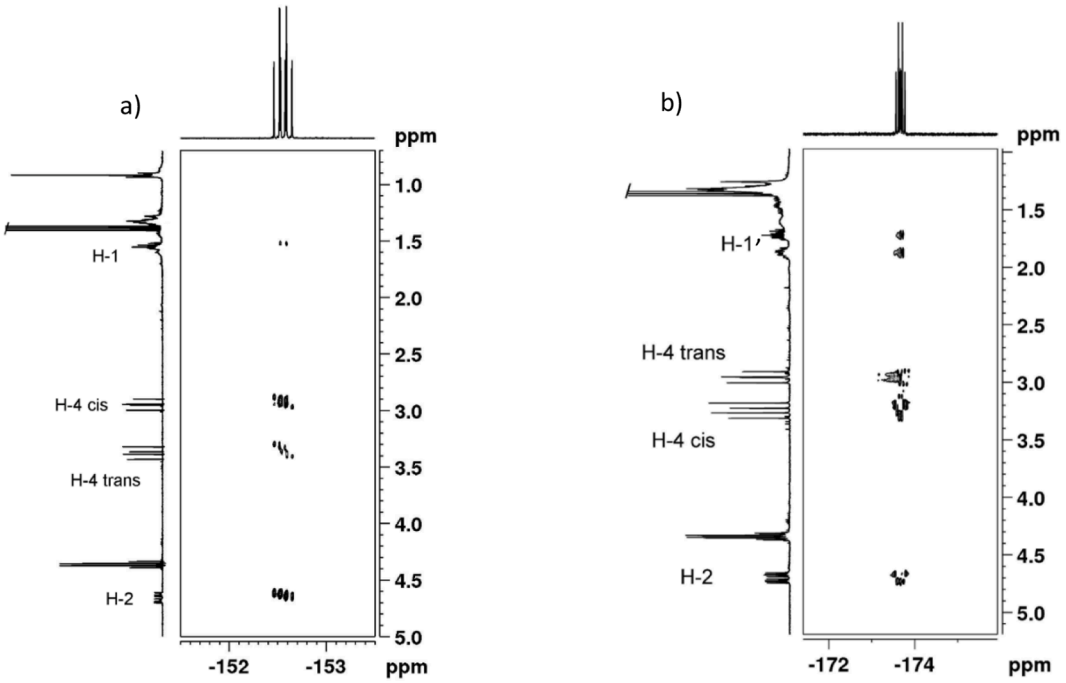

Figure 1. a) $^{19}F\{^{1}H\}$-HOESY NMR spectrum (376.65 MHz, 298K, $CDCl_3$, 200mM) of **6b**; b) $^{19}F\{^{1}H\}$-HOESY NMR spectrum of **7b**.

images pair E_3 (2*S*,3*R*) and ^3E (2*R*,3*S*) and with F pseudo-equatorial any member of the pair ^3E (2*S*,3*R*) and E_3 (2*R*,3*S*). For **7** F pseudo-axial conformation corresponds to ^3E for (2*S*,3*S*) and E_3 (2*R*,3*R*) and F pseudo-equatorial conformation to E_3 (2*S*,3*S*) and ^3E (*2R,3R*) (Figure 2).

The presence of the rigid ester group imposes a planar constraint which allows just the two envelope conformations whereas the presence of substituents on the γ-lactone ring modulates the relative populations [31,32].

The conformers generated by the open source software RDKit [47, 48], after energy minimization, clustered around the two ^3E and E_3 envelope conformations.

The energy values obtained through molecular mechanics based methods must be considered with caution, being not extremely accurate [49], but in the case of substituted paraconic esters proved rather reliable [32].

For the present compounds, interesting suggestions emerge from the analysis of the energy data.

Considering the lowest energy structures for the F pseudo-axial and F pseudo-equatorial conformations for both molecules, it appears that the pseudo-axial (E_3) conformation of (2*R*,3*R*)-**7a** is the most stable one. It is about 9 kJ/mol lower in energy than the F pseudo-equatorial, ^3E, one of the same molecule, indicating that in the case of this diastereomer there is a by far more abundant conformer. Both conformers of (2*R,3S*)-**6a** are higher in energy than the **7a** conformers. Moreover, they are close in energy, only about 0.7 kJ/mol apart, with the population of the F pseudo-axial ^3E conformer somewhat higher than that of the F pseudo-equatorial E_3.

The geometry of these two pairs of conformers of the diastereomers **6a** and **7a** were then optimized using DFT. A conformational search applied to the ethyl esters derivatives gave similar results and the geometry of the conformers with lower energy has been optimized at the DFT level as well as for compounds **10** and **11**.

The DFT optimized Cartesian coordinates for all conformers are listed in the SI (Tables S20-S27 and S38-S41), and the optimized

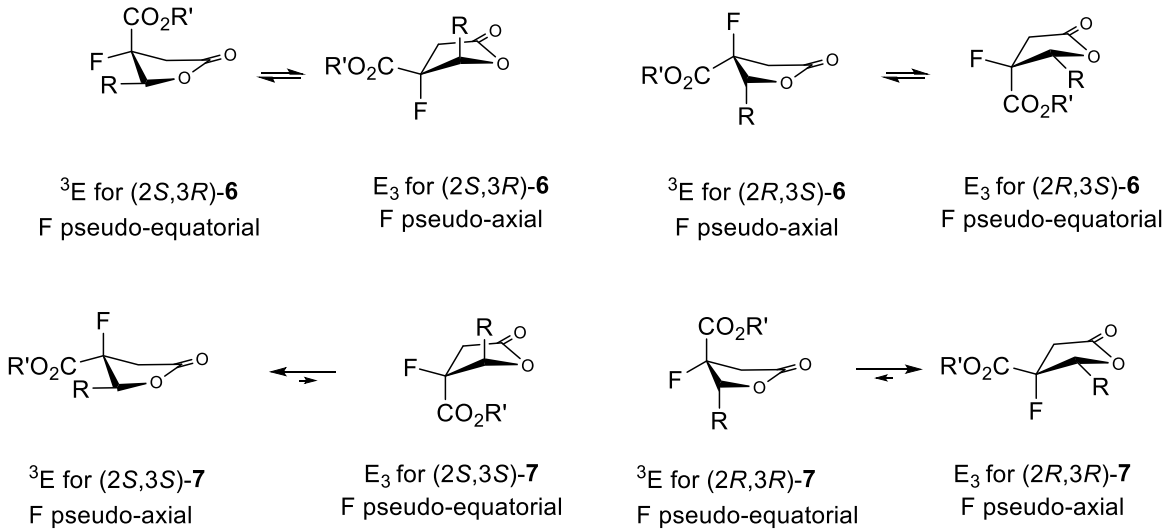

Figure 2. Conformational equilibria for racemic mixtures of lactones **6** and **7**.

geometries are reported in Figures 3 (compounds **7a** and **6a**), S7 (compounds **7b** and **6b**), and S8 (compounds **10** and **11**). For each conformer, the relative energy (in kJ/mol) including zero-point corrections (ZPVE), the natural charge on the F atom derived from natural population analysis, and computed shifts (both unscaled and scaled according to Eq. (3), see Experimental) are reported in Table 1 for the conformers of **6a** and **7a**, in Table S3 for **6b** and **7b** and in Table S28 for **10** and **11**.

An analysis of computed relative energies (enthalpies at T=0K, *in vacuo*) suggests that the conformers of **7a** and **7b** are more stable than the corresponding ones of **6a** and **6b**. However, by inspecting their relative Gibbs free energies at 298 K, one sees that the stability of **6a** and **7a** is comparable. This is at variance with what found for compounds **10** and **11**, where the trend in relative Gibbs free energies parallel that of the total energies (see Table S28 in the SI). This is in agreement with earlier DFT conformational analysis on paraconic acid carried out both in vacuum and with implicit solvent (methanol) [50].

The optimized geometries of the two conformers of the (2*R*,3*R*)-**7a** differ mainly by the torsional angles of the lateral chains, while sharing the same puckering conformation of the 5-membered γ-lactone ring. This is at variance with the two low-energy conformers of (2*R*,3*S*)-**6a** which also keep the different conformations of the γ-lactone ring (see the C4-C3-C2-O1 dihedral angle values, Table S2). A similar analysis applies to the optimized geometries of the low-energy conformers identified for (2*R*,3*R*)-**7b** and (2*R*,3*S*)-**6b** (see Table S2, and Figure S7) and for (2*R*,3*R*)-**11** and (2*R*,3*S*)-**10** (see Figure S8).

The analysis of the optimized DFT geometries reveals that the orientation of the F-C and C=O bond dipoles is almost antiparallel for the conformers of diastereomers **7** and **11** (the corresponding dihedral angle approaches the ideal value of 180°) while the corresponding dihedral angle is appreciably lower than 180° for the conformers of diastereomers **6** and **10** (150-160°)

2.4. NBO/NLMO analysis of computed ^{19}F NMR chemical shifts

For a closed-shell molecule with N electrons, there will be N/2 doubly occupied scalar relativistic MOs (and correspondingly N singly occupied two-component spinors). These canonical MOs are usually delocalized. One can obtain the same Kohn-Sham density matrix (and therefore electron density) with a set of localized orthonormal MOs. For the purpose of analyzing the results of NMR calculations, we used natural localized molecular orbitals (NLMOs) based on the localization criterium of Weinhold et al. [51-53]. This set of N/2 occupied spin-free NLMOs can be written as a linear combination of strongly localized natural bonding orbitals (NBOs), which can be thought as a quantum mechanical analog of a molecular Lewis structure. If the linear combination is written as:

$$\phi_j^{NLMO} = \Omega_j W_{jj} + \sum_{i \neq j}^{NBO} \Omega_i^{NBO} W_{ij} \quad (1)$$

Ω_j being the strongly localized "parent" NBO, the first term of the right-hand side of Eq. (1) is called the Lewis part (L) of the NLMO, while the summation of the right-hand side represents the delocalization tail of the *j*-th NLMO, and will be termed non-Lewis (NL) in the analysis below. In the NLMO's analysis of the ^{19}F isotropic shielding, the diamagnetic (d) and paramagnetic+SO (p+SO) contributions have both L and NL parts, and their analysis can give an indication of the degree of deviation of the valence electron distribution from an idealized Lewis picture. NBOs can in fact be classified as core orbitals, non-bonding electron pairs (LP), bonding orbitals (BD), antibonding orbitals (BD*), and Rydberg orbitals. The degree of delocalization shows up also in a set of NBOs with low occupancy, and with occupations of the dominant N/2 set of NBOs significantly below 2 [54]. NBO/NLMO analysis of computed ^{19}F shielding contributions are reported in Tables S4-S19 of the SI.

Focusing on computed ^{19}F NMR shielding for the conformers with R = CH_3 (a similar analysis can be carried out for the four low-energy conformers with R = CH_2CH_3, see Table S3), reported in Table 1, one notices that the two **7a** conformers, with the same kind of ring puckering, present a very similar value for σ_F (around 339-340 ppm). Lower values are predicted for the **6a** conformers. Actually, for the two low-energy ^{3}E and E_3 conformations of **6a** and **6b** characterized in this work there is a somewhat larger difference (of about 8-10 ppm) between computed σ_F values, and whose origin will be investigated at the end of this section. Our primary task here is to get a qualitative insight into the origin of the computed ^{19}F deshielding of about 30 ppm found in going from the (2*R*,3*R*)-**7a** E_3 to the (2*R*,3*S*)-**6a** ^{3}E. The observed trend in chemical shift cannot be rationalized by a simple inspection of the F natural charge (Q_F in Table 1). This is in line with previous DFT works [55,56]. To shed some light on the origin of the observed and calculated trend, we first inspect the results of the isotropic shielding analysis carried out in term of NLMOs, and reported in full in Tables S4 and S5 for conformers (2*R*,3*R*)-**7a** E_3 and Tables S6 and S7 for (2*R*,3*S*)-**6a** ^{3}E and E_3, respectively. In doing so, we focus on the p+SO contributions, since the diamagnetic part, dominated by the contributions of F core and lone pairs (LPs), varies little along the series of conformers. The p+SO contributions can further be broken down in contributions from *i*) the F core orbital (whose value is however similar for both conformers and will not be considered further), *ii*) O LPs of the COOR residue, *iii)* F LPs, further classified by symmetry into σ (directed along the C-F bond) and π components, and *iv)* contributions from C-H σ bonds of C atoms adjacent to the C-F bond and C-C σ bonds involving the C atom directly bonded to the F center, as can be seen from an inspection of Tables S4-S7.

Figures 4a-c report a graphical representation of the columns of Tables S4-S11 and S30-33 reporting the p+SO contributes to shielding as incremental sums, so that the last point is the total contribution to shielding. The order reflects the magnitude of the L contributions.

While the major contributions to the p+SO shielding are due, in both ring conformers, to the F LPs, their different magnitude alone cannot explain the observed ^{19}F deshielding of about 30 ppm found in going from (2*R*,3*R*)-**7a** E_3 to (2*R*,3*S*)-**6a** ^{3}E. This difference is rather the combination of the above with C-H and C-C σ bonds contributions that change sign in going from the **7a** to the **6a** configuration, together with a stronger shielding effect of the C-F σ bond in **6a** compared to **7a**. The fact that the occupation of the relevant NLMOs, which deviates quite

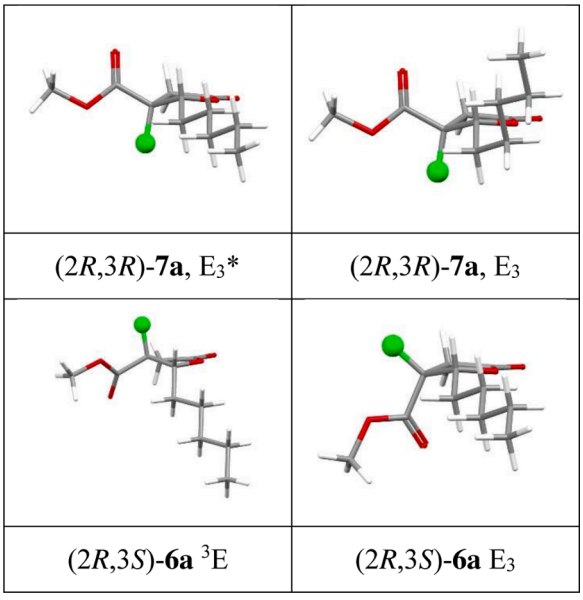

Figure 3. Optimized geometries of the four (2*R*,3*S*)-**6a** and (2*R*,3*R*)-**7a**, ^{3}E and E_3 conformers computed at the DFT ZORA TZ2P/BLYP level. * Starting from ^{3}E conformation.

Table 1
Computed relative energies (ΔE, including ZPVE), Gibbs free energies, Fluorine natural charge (Q_F, in units of the elementary charge, *e*), isotropic shielding (σ_F) together with the diamagnetic (σ_d) and paramagnetic plus SO terms (σ_{p+SO}), and computed (scaled) chemical shifts, for the conformers with R = CH_3.

conformer	ΔE (kJ/mol)	ΔG (kJ/mol)	Q_F	σ_d (ppm)	σ_{p+SO} (ppm)	σ_F (ppm)	$\delta_{calc.}$[a] (ppm)
(2*R*,3*R*)-**7a** E_3[b]	0.0	0.05	-0.36327	476.4	-137.6	338.8	-174.7
(2*R*,3*R*)-**7a** E_3	3.94	4.01	-0.36355	476.5	-136.4	340.1	-175.8
(2*R*,3*S*)-**6a** ^3E	5.37	0.00	-0.36665	477.1	-171.4	305.6	-145.8
(2*R*,3*S*)-**6a** E_3	9.76	3.72	-0.36362	476.6	-161.4	315.2	-154.1

[a] Calculated according to Eq. (3) in the Experimental. [b] Starting from an ^3E conformation.

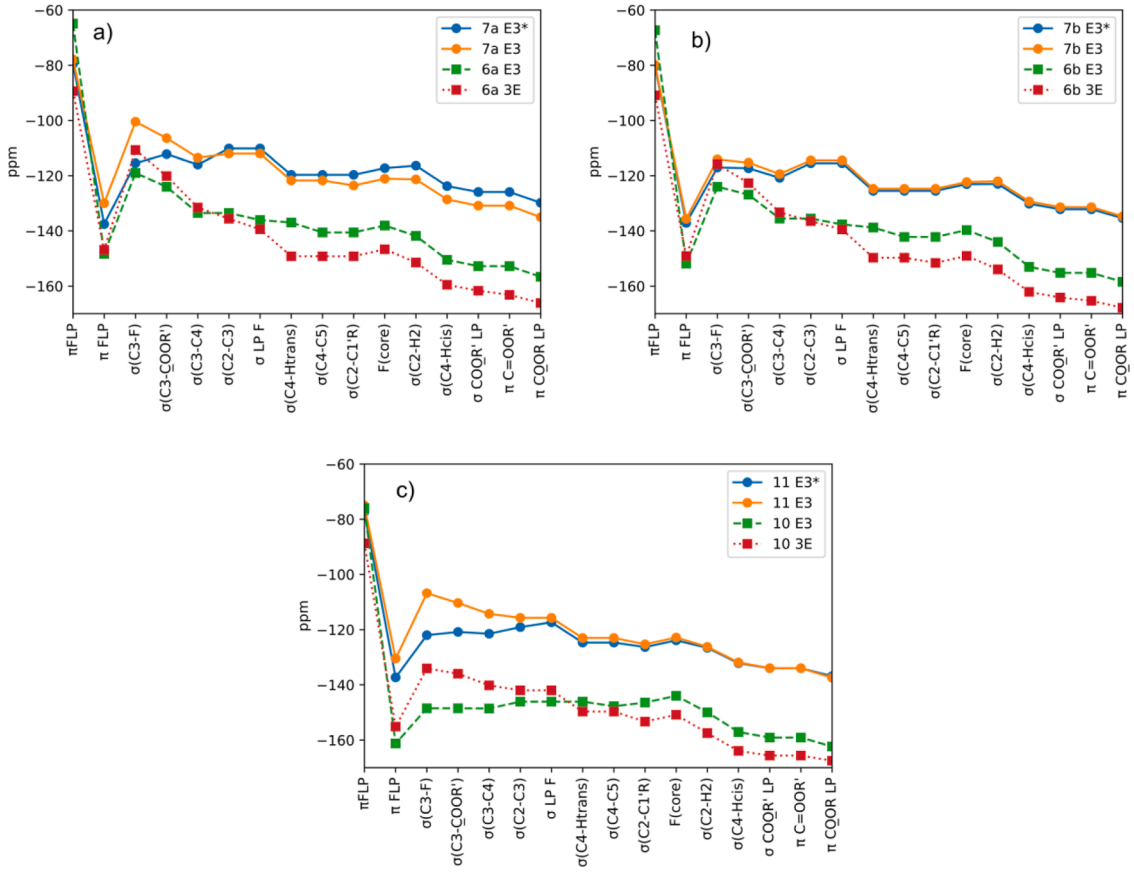

Figure 4. Incremental sums of p+SO contributions for compounds: a) **7a** and **6a** (see Tables S4-S7), b) **7b** and **6b** (see Tables S8-S11) and c) **10** and **11** (Tables S30-S33).

significantly from the value of 2 in most cases, and notably also for F LPs, indicates non-negligible electron delocalization effects. Effects of electron delocalization are also apparent from the corresponding NBOs analysis, reported in Tables S12 and S14-S15, and in particular from the contribution of antibonding orbitals, notably the σ*(C-F). Here the analysis parallels that done above in terms of NLMOs. A similar NLMOs/NBOs analysis can also be used to rationalize the small difference of computed ^{19}F shielding between the two **6a** conformers. This is a results of differences among the magnitudes of C-H, C-C, and C-F σ bonds contributions. Selected NLMOs/NBOs for the two configurations are reported in Figure 5. The trend in computed ^{19}F shieldings found for the **7b** and **6b** configurations can be discussed along similar lines.

To further supplement the analysis of the NBOs contributions to the ^{19}F shielding, we report in Table 2 selected electron delocalization interactions (such as σ→σ*), based on second order perturbation theory analysis of the Kohn-Sham matrix in the NBO basis.

The chemical shielding calculations carried out on compounds **10** and **11** corroborate the results obtained for compounds **6** and **7**.

Finally, the introduction of fluorine did not cause any dramatic changes concerning structure and preferred conformations, as revealed by the comparison of the geometries calculated for **6a** and **7a** and the parent not fluorinated lactones *cis* and *trans*-**14** [57] (see Figure S11) and those of **10** and **11** with literature results for *cis* and *trans*-**13** [58] (Figure 6).

3. Conclusion

The preparation of β-fluorinated paraconic acid derivatives has been conveniently accomplished by lactonization, after reduction, of methyl and ethyl acylsuccinate fluorinated by Selectfluor. The reduction in acidic medium and the acidic treatment of the silica, used as stationary phase for chromatographic separation, suppressed the HF elimination reaction to a great extent.

The product was isolated as a pair of diastereomers, possessing two chiral carbons. It is interesting to notice that a carbon-fluorine quaternary stereogenic center was formed [59] and this is a stimulating result in the perspective of achievement of enantiomerically pure final products e.g. either by asymmetric metal catalyzed fluorination [22] or by asymmetric reduction [18].

The stereochemistry of each diastereomer was assessed by NMR

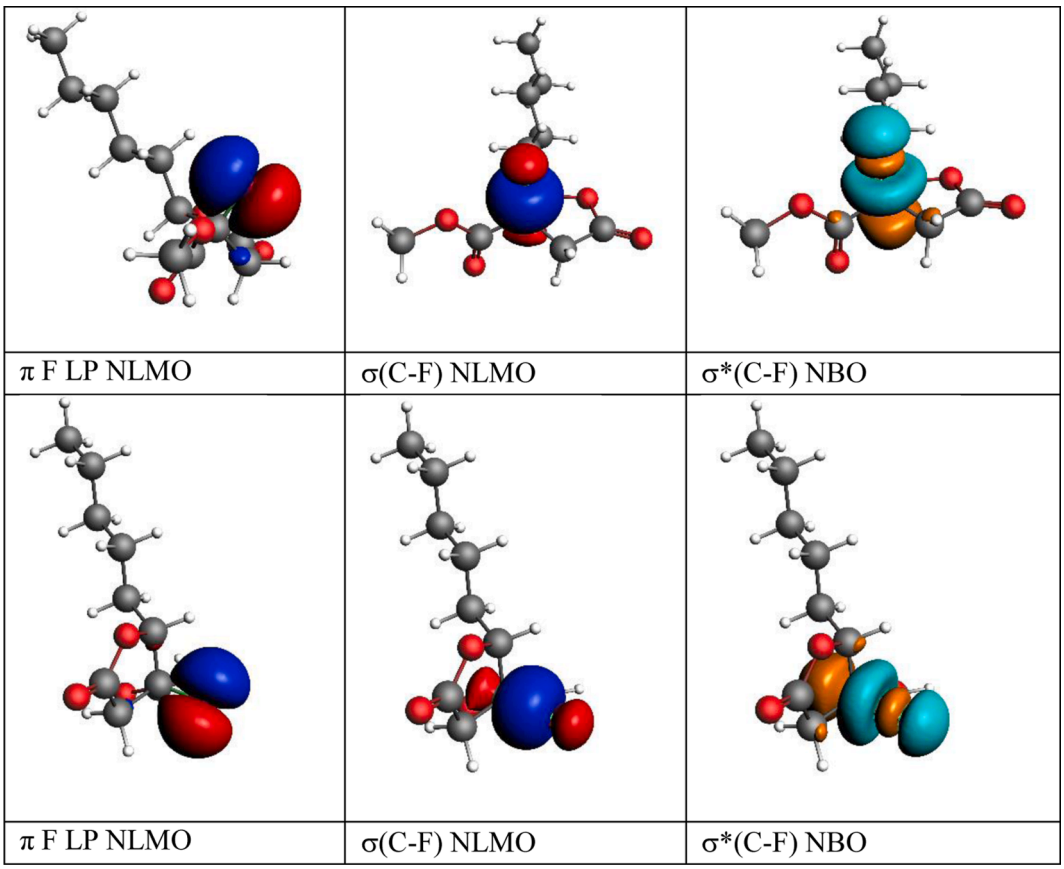

Figure 5. Plot of selected NLMOs/NBOs for (2*R*,3*R*)-**7a** E_3 with lower energy (top row) and (2*R*,3*S*)-**6a** ^3E (bottom row). In all cases the MOs are plotted with an isovalue of 0.03.

spectroscopy through ^1H-^{19}F heteronuclear Overhauser effect and thus the ^{19}F NMR signals unambiguously assigned. This allows the use of a simple 1D ^{19}F NMR spectrum as a diagnostic tool for the identification of the diastereomers, being the shift difference 20 ppm.

On the basis of molecular mechanics conformational analysis and relativistic DFT calculations, it appears that the introduction of fluorine does not heavily affect the conformational equilibrium of the puckering of the lactone ring.

To get insight into the observed ^{19}F chemical shift difference for the two diastereomer, we applied a NBO/NLMO decomposition analysis of computed ^{19}F nuclear shielding. Although it proves difficult to correlate the observed dependence of ^{19}F NMR shielding on stereochemistry to a small number of localized orbitals and/or electron interactions, the important role of electron-delocalization effects (hyperconjugative interaction), also revealed from a perturbative analysis of interaction energies, appears quite clear.

4. Experimental

4.1. General methods

IR spectra were recorded on a Thermo Nicolet AVATAR 320 FT/IR spectrophotometer. ^1H-NMR and ^{13}CNMR spectra were run on a Varian 400MR and on a Bruker AVANCE IIIHD spectrometers both operating at 400 MHz for proton, 101 MHz for carbon and 376 MHz for fluorine, on a Varian 500VNMRS spectrometer, using deutero chloroform as a solvent and TMS as the internal standard. Coupling constants are given in Hz. NMR data were processed by MestReNova 10.0. $^{19}F\{^1H\}$-HOESY NMR spectra were acquired using the standard four-pulse sequence [60]. The number of transients and data points was chosen according to the sample concentration and desired final digital resolution. Semi-quantitative spectra were acquired using a 2s relaxation delay and 700 ms mixing times. High resolution mass spectra (HRMS) were recorded on a micrOTOF-Q – Bruker instrument. Exact masses were calculated by enviPat Web 2.2 (http://www.envipat.eawag.ch/index.php) [61]. Microwave irradiations were performed by a CEM Discover System instrument. TLC's were performed on Polygram Sil G/UV254 silica gel pre-coated plastic sheets (eluent: light petroleum-ethyl acetate). Flash chromatography was run on silica gel 230-400 mesh ASTM (Kieselgel 60, Merck, Darmstadt, Germany). Light petroleum refers to the fraction with b.p. 40–70°C and ether to diethyl ether. Dimethyl acetylsuccinate was purchased from Sigma-Aldrich, dimethyl and diethyl hexanoylsuccinates **1a** [36] and **1b** [25] were prepared by radical addition of hexanal to dimethyl or diethyl maleate according to the literature [35].

4.2. Fluorination of hexanoyl succinate *1a* under microwave irradiation

In a tube (10 mL) for microwave irradiation, equipped with a teflon coated stirring bar, to **1a** (0.250 g, 1.02 mmol) dissolved in 6 mL of a mixture of CH_3CN : H_2O (4 :1), Selectfluor® (0.700 g, 2.00 mmol) was added under stirring. The temperature was set to 80°C and irradiated for 4 h. The reaction was followed by TLC (light petroleum : ethyl acetate, 80 : 20 v/v, visualised with I_2 vapour and then by treatment with an acidic solution of $KMnO_4$). After evaporation of the solvent water was added and extracted 5 times with ether. The organic phases were washed with water and brine, then dried on anhydrous Na_2SO_4. Evaporation of the solvent afforded a crude reaction mixture which was purified by flash chromatography (ethyl acetate-light petroleum, gradient from 2% up to 7%). Compound **2a** (0.200 g, 0.76 mmol) was isolated in 44% yield.

1,4-Dimethyl 2-fluoro-2-(1-oxohexyl)-butanedioate 2a

Table 2
Selected NBO $E^{(2)}$ energies (kcal/mol) for conformers (2*R*,3*R*)-**7a** E_3[a], (2*R*,3*S*)-**6a** ^3E and (2*R*,3*S*)-**6a** E_3. Only $E^{(2)}$ energies larger than 0.5 kcal/mol are included.

donor NBO	acceptor NBO	(2*R*,3*R*)-**7a** E_3[a]	(2*R*,3*S*)-**6a** ^3E	(2*R*,3*S*)-**6a** E_3
		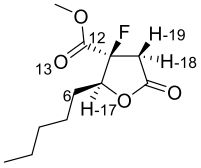	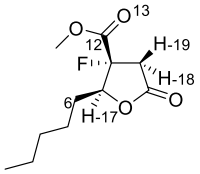	
n(F, σ)	Ryd. (C3)	7.77	7.52	8.12
n(F, π_1)	σ*(C2-C3)	3.31	4.41	6.20
n(F, π_1)	σ*(C3-C4)	5.54	4.14	1.77
n(F, π_1)	σ*(C3-C12)	0.59		1.54
n(F, π_1)	σ*(O1-C2)			0.77
n(F, π_1)	Ryd(C3)	1.59	2.01	1.97
n(F, π_2)	σ*(O13-C12)	0.53		
n(F, π_2)	π*(O13-C12)		0.57	
n(F, π_2)	σ*(C2-C3)	3.57	1.56	
n(F, π_2)	σ*(C3-C12)	7.28	7.08	6.15
n(F, π_2)	σ*(C3-C4)		1.43	4.45
n(F, π_2)	Ryd(C3)	1.49	1.86	2.07
σ (C3-F)	σ*(O13-C12)	0.99	0.86	0.93
σ (C3-F)	π*(O13-C12)		0.64	
σ (C3-F)	σ*(O1-C2)			0.53
σ (C3-F)	σ*(C2-C6)		0.73	
σ (C3-F)	σ*(C4-H18)	0.53		
σ (C3-F)	σ*(C4-H19)		0.56	
n(O13, π)	σ*(C3-F)	0.94	0.62	0.77
σ(O13-C12)	σ*(C3-F)	0.53		
σ(O1-C2)	σ*(C3-F)			0.91
π(O13-C12)	σ*(C3-F)		1.10	0.54
σ(C2-C6)	σ*(C3-F)	0.71	1.46	
σ(C2-H17)	σ*(C3-F)	3.09	2.15	2.05
σ(C4-H18)	σ*(C3-F)	2.93	1.97	
σ(C4-H19)	σ*(C3-F)	1.88	3.12	2.36
σ(C4-C5)	σ*(C3-F)			1.86

[a] Starting from an ^3E conformation.

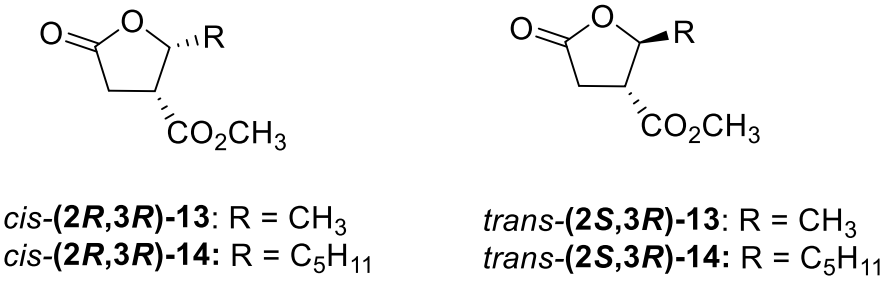

Figure 6. Structures of not fluorinated lactones **13** and **14**.

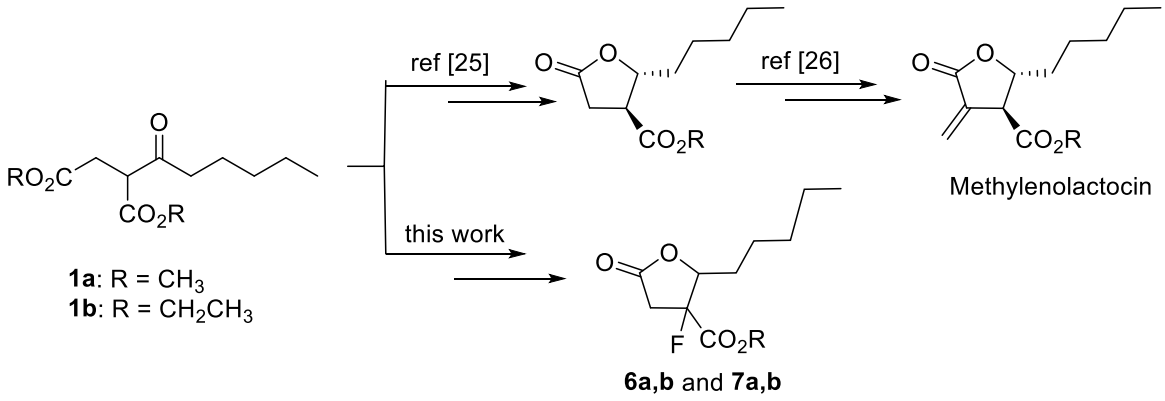

Scheme 1. The strategy for the preparation of fluorinated lactones **6** and **7**.

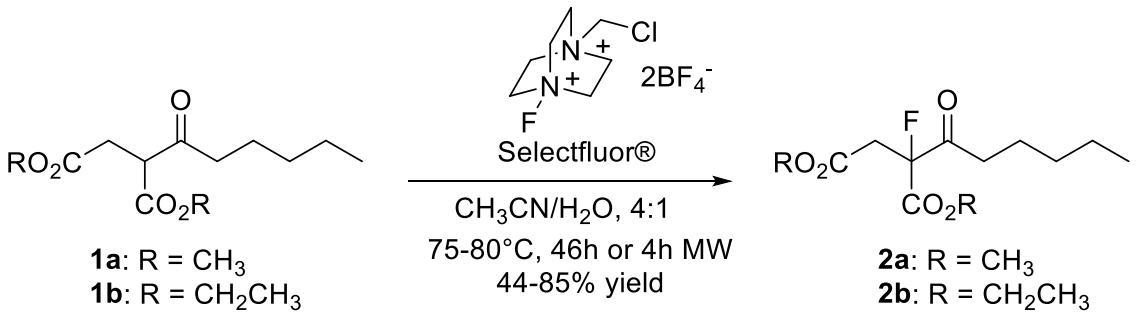

Scheme 2. Synthesis of fluorinated succinates **2**.

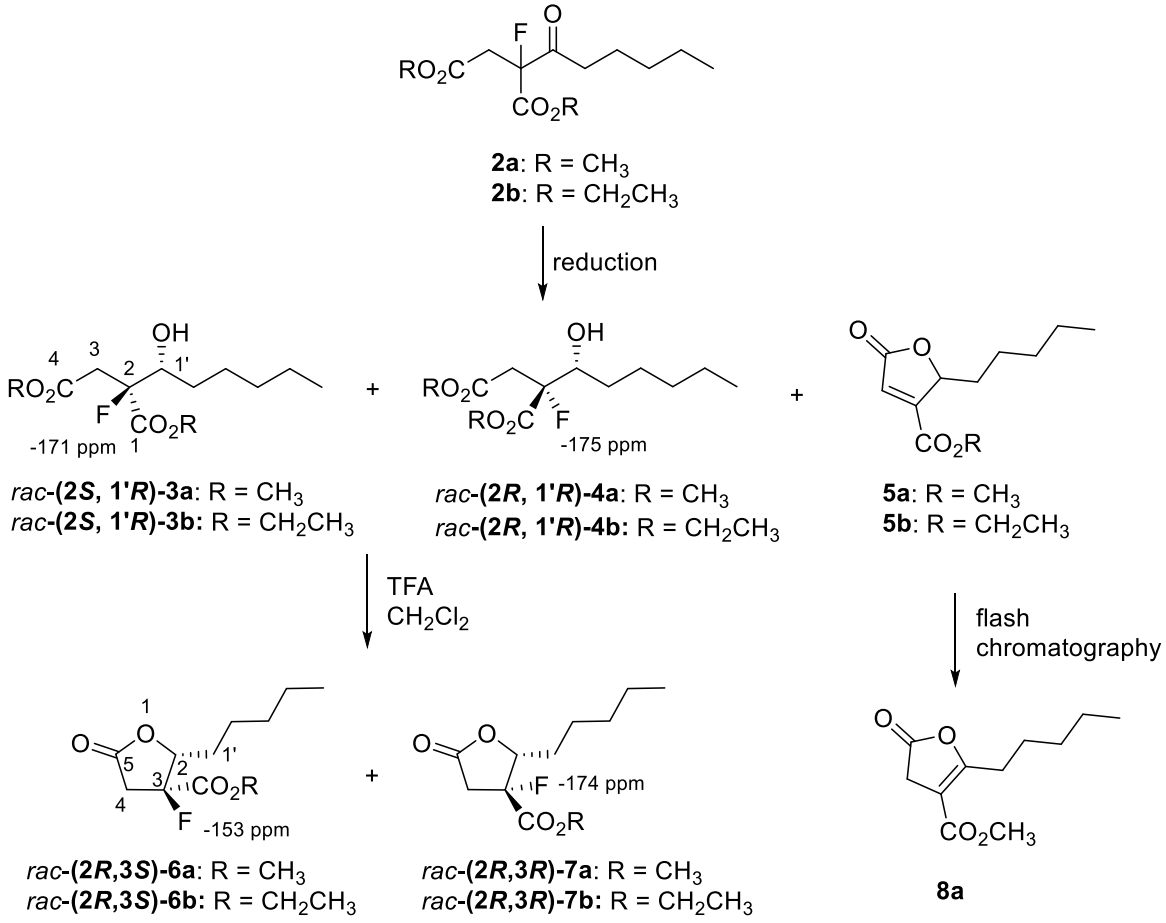

Scheme 3. Synthesis of lactones **6** and **7**.

Oil. Yield = 44%. ^{1}H NMR (400 MHz, $CDCl_3$): δ 3.82 (s, 3H, OCH_3), 3.70 (s, 3H, OCH_3), 3.32, 3.21 (AB part of an ABX system, 2H, $^{2}J_{HH}$ = 17.5 Hz, $^{3}J_{HF}$ = 19.9 Hz, $^{3}J_{HF}$ = 27.5 Hz, H-3), 2.86 (dtd, 1H, $^{2}J_{HH}$ = 18.6 Hz, $^{3}J_{HH}$ = 7.3 Hz, $^{4}J_{HF}$ = 3.9 Hz, CH_2COCF), 2.69 (dtd, 1H, $^{2}J_{HH}$ = 18.6 Hz, $^{3}J_{HH}$ = 7.3 Hz, $^{4}J_{HF}$ = 2.6 Hz, CH_2COCF), 1.61 (quintet, 2H, $^{3}J_{HH}$ = 7.3 Hz, CH_2), 1.31 (m, 4H), 0.89 (t, 3H, $^{3}J_{HH}$ = 7.0 Hz, CH_3). ^{19}F NMR (376 MHz, $CDCl_3$): δ -166.66 – -166.82 (m). ^{13}C NMR (101 MHz, $CDCl_3$): δ 204.02 (d, ^{2}J = 27.2 Hz, C-1'), 168.72 (s, C-4), 165.90 (d, ^{2}J = 25.0 Hz, C-1), 97.50 (d, ^{1}J = 201.6 Hz, C-2), 53.74 (s, OCH_3), 52.41 (s, OCH_3), 39.32 (d, ^{2}J = 22.1 Hz, C-3), 37.73 (s), 31.18 (s), 22.53 (s), 22.46 (d, ^{4}J = 1.6 Hz, C-3'), 14.03 (s, CH_3). IR (film, cm^{-1}): 1750.6. HRMS (ESI) m/z: calcd for $C_{12}H_{19}FO_5Na^{+}$ $[M+Na]^{+}$ 285.1109, found 285.1110.

4.3. Fluorination of acylsuccinates by conventional heating

To the acylsuccinate (6.22 mmol) dissolved in 25 mL of a CH_3CN : H_2O (2:1 or 4:1) mixture, Selectfluor® (4.77 g, 13.43 mmol) was added. The mixture was heated at 75°C for 20 h under stirring, then another portion of Selectfluor® (2.79 g, 7.8 mmol) was added and the solution was heated at 80°C for another 8 h, this addition was not necessary for the fluorination of dimethyl acetylsuccinate. The reaction was allowed to stand for 18 h with stirring at room temperature. The progress of the reaction was monitored by TLC. After evaporation of the solvent, water was added and extracted 5 times with ether. The organic phases were washed with brine and dried on anhydrous Na_2SO_4. Evaporation of the solvent gave the corresponding fluorinated acylsuccinate. Compound **9** was isolated in 74% yield after purification by flash chromatography, compound **2b** (1.543 g, 5.28 mmol, 85% yield) didn't need further

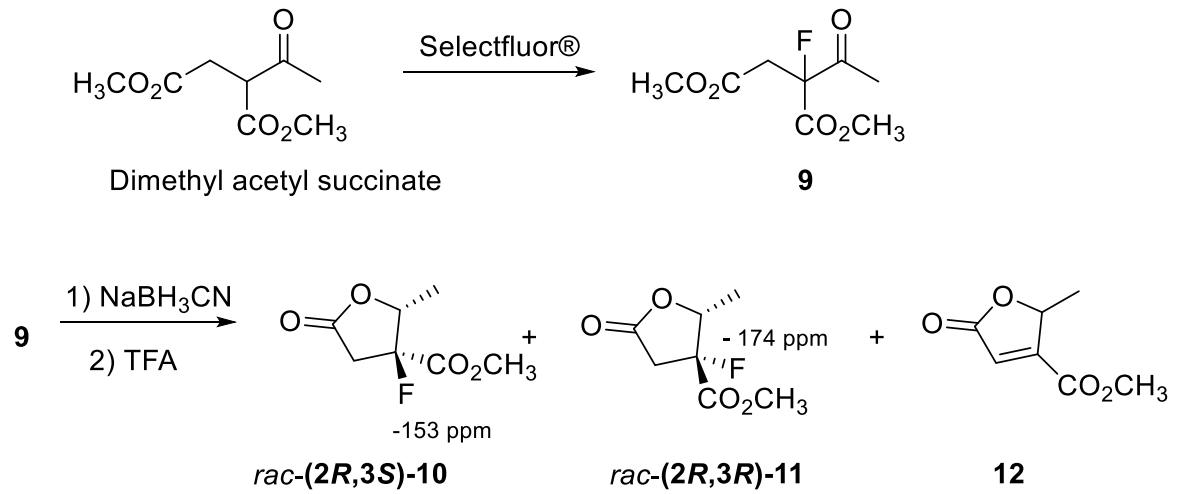

Scheme 4. Synthesis of lactones **10** and **11**.

purification.

1,4-Diethyl 2-fluoro-2-(1-oxohexyl)-butanedioate 2b

Oil. Yield = 85%. ^{1}H NMR (400 MHz, $CDCl_3$): δ 4.33 – 4.21 (m, 2H, OCH_2CH_3), 4.14 (q, 2H, $^{3}J_{HH}$ = 7.2 Hz, OCH_2CH_3), 3.30, 3.19 (AB part of an ABX system, 2H, $^{2}J_{HH}$ = 17.4 Hz, $^{3}J_{HF}$ = 19.8 Hz, $^{3}J_{HF}$ = 27.6 Hz, H-3), 2.89 – 2.77 (m, 1H, CH_2COCF), 2.75 – 2.64 (m, 1H, CH_2COCF), 1.60 (quintet, 2H, $^{3}J_{HH}$ = 7.2 Hz, CH_2), 1.37-1.23 (m, 4H), 1.29 (t, 3H, $^{3}J_{HH}$ = 7.1 Hz, OCH_2CH_3), 1.24 (t, 3H, $^{3}J_{HH}$ = 7.2 Hz, OCH_2CH_3), 0.88 (t, 3H, $^{3}J_{HH}$ = 6.9 Hz, CH_3). ^{19}F NMR (376 MHz, $CDCl_3$): δ -166.65 – -166.81 (m). ^{13}C NMR (101 MHz, $CDCl_3$): δ 204.10 (d, ^{2}J = 27.3 Hz, C-1'), 168.23 (s, C-4), 165.42 (d, ^{2}J = 24.9 Hz, C-1), 97.53 (d, ^{1}J = 201.1 Hz, C-2), 63.04 (s, OCH_2CH_3), 61.45 (s, OCH_2CH_3), 39.48 (d, ^{2}J = 22.0 Hz, C-3), 37.70 (s), 31.19 (s), 22.51 (2s), 14.15 (s, CH_3), 14.03 (s, CH_3), 13.99 (s, CH_3). IR (KBr, cm^{-1}): 1741.6. HRMS (ESI) m/z: calcd for $C_{14}H_{23}FO_5Na^+$ $[M+Na]^+$ 313.1422, found 313.1423.

1,4-Dimethyl 2-acetyl-2-fluorobutanedioate 9

Oil. Yield = 74%. ^{1}H NMR (400 MHz, $CDCl_3$) δ 3.82 (s, 3H, OCH_3), 3.69 (s, 3H, OCH_3), 3.33, 3.20 (AB part of an ABX system, 2H, $^{2}J_{HH}$ = 17.5 Hz, $^{3}J_{HF}$ = 19.0 Hz, $^{3}J_{HF}$ = 28.3 Hz, H-3), 2.41 (d, 3H, $^{4}J_{HF}$ = 5.1 Hz, CH_3). ^{19}F NMR (376 MHz, $CDCl_3$) δ -164.34 (ddq, $^{3}J_{HF}$ = 28.3, $^{3}J_{HF}$ = 19.0, $^{4}J_{HF}$ = 5.1 Hz). ^{13}C NMR (101 MHz, $CDCl_3$) δ 202.10 (d, ^{2}J = 28.9 Hz, CO), 168.68 (s, C-4), 165.68 (d, ^{2}J = 24.9 Hz, C-1), 97.31 (d, ^{1}J = 201.6 Hz, C-2), 53.82 (s, OCH3), 52.45 (s, OCH3), 39.22 (d, ^{2}J = 22.0 Hz, C-3), 25.74 (d, ^{3}J = 0.6 Hz, CH_3). IR (film, cm^{-1}): 1732.1. HRMS (ESI) m/z: calcd for $C_8H_{11}FO_5Na^+$ $[M+Na]^+$ 229.0483, found 229.0482.

*4.4. Reduction of ketodiester **2a** with $NaBH_4$*

To compound **2a** (0.137 g, 0.52 mmol) dissolved in 2.5 mL of MeOH, $NaBH_4$ (0.010 g, 0.26 mmol) was added under stirring. The progress of the reaction was monitored by TLC, after 1 h, the solvent was evaporated, water was added and extracted with ether. Organic phases were dried on anhydrous Na_2SO_4. After evaporation of the solvent the crude reaction mixture was purified by flash chromatography (ethyl acetate-light petroleum, gradient from 3% up to 15%). Hydroxydiester **3a (**0.035 g, 0.15 mmol, 25% yield), butenolide **5a** (0.010 g, 0.047 mmol, 9% yield) and its isomer **8a** (0.05 g, 0.023 mmol, 4% yield) were isolated.

***rel*-1,4-Dimethyl (2*S*)-2-fluoro-2-[(1*R*)-1-hydroxyhexyl]-butanedioate 3a**

Oil. Yield = 25%. ^{1}H NMR (400 MHz, $CDCl_3$): δ 3.87 (s, 3H, OCH_3), 3.76 (m, 1H, C*H*OH), 3.71 (s, 3H, OCH_3), 3.20 (dd, 1H, $^{3}J_{HF}$ = 36.0, $^{2}J_{HH}$ = 16.6 Hz, H-3), 2.92 (dd, 1H, $^{2}J_{HH}$ =16.6, $^{3}J_{HF}$ = 10.2 Hz, 1H, H-3), 2.10 (dd, 1H,$^{3}J_{HH}$ = 9.2, $^{4}J_{HF}$ = 1.1 Hz, OH), 1.58 (m, 2H), 1.32 (m, 6H), 0.89 (t, 3H, $^{3}J_{HH}$ = 6.8 Hz, CH_3). ^{19}F NMR (376 MHz, $CDCl_3$) δ -171.58 (m). ^{13}C NMR (101 MHz, $CDCl_3$): δ 170.45 (d, ^{2}J = 24.5 Hz, C-1), 169.34 (s, C-4), 96.50 (d, ^{1}J = 194.7 Hz, C-2), 74.43 (d, ^{2}J = 24.4 Hz, CHOH), 53.02 (s, OCH_3), 52.36 (s, OCH_3), 38.84 (d, ^{2}J = 23.1 Hz, C-3), 31.64 (s, C-2'), 31.07 (d, ^{4}J = 2.3 Hz, C-3'), 25.53 (s), 22.65 (s), 14.13 (s, CH_3). IR (film, cm^{-1}): 3469 (OH),1745 (COO). HRMS (ESI) m/z: calcd for $C_{12}H_{21}FO_5Na^+$ $[M+Na]^+$ 287.1265, found 287.1269.

Methyl 5-oxo-2-pentyl-2,5-dihydrofuran-3-carboxylate 5a

Oil. Yield = 9%. ^{1}H NMR (400 MHz, $CDCl_3$): δ 6.65 (d, 1H, ^{4}J = 2.0 Hz, H-4), 5.22 (ddd, 1H, ^{3}J = 8.1, ^{3}J = 3.1, ^{4}J = 2.0 Hz, H-2), 3.89 (s, 3H, OCH_3), 2.12 (m, 1H), 1.63 (m, 1H), 1.50 – 1.16 (m, 6H), 0.89 (t, 3H, ^{3}J = 6.9 Hz). ^{13}C NMR (101 MHz, $CDCl_3$) δ 171.13 (s, C-5), 161.60 (s, COO), 157.45 (s, C-3), 127.05 (d, C-4), 82.77 (d, C-2), 52.96 (q, OCH_3), 32.62 (t), 31.47 (t), 24.52 (t), 22.52 (t), 14.08 (q, CH_3). IR (film, cm^{-1}): 1766, 1733, 1634. HRMS (ESI) m/z: calcd for $C_{11}H_{16}O_4Na^+$ $[M+Na]^+$ 235.0941, found 235.0942.

Methyl 5-oxo-2-pentyl-4,5-dihydrofuran-3-carboxylate 8a [38].

Oil. ^{1}H NMR (400 MHz, $CDCl_3$): δ 3.77 (s, 3H, OCH_3), 3.44 (t, 2H, ^{5}J = 1.6 Hz, H-4), 2.81 (m, 2H, H-1'), 1.63 (m, 2H), 1.34 (m, 4H), 0.90 (t, 3H, ^{3}J = 7.1 Hz,). ^{13}C NMR (101 MHz, $CDCl_3$) δ 173.16 (s), 167.68 (s), 163.60 (s), 105.64 (s, C-3), 51.73 (q, OCH_3), 33.85 (d, C-4), 31.38 (t), 27.42 (t, C-1'), 26.23 (t), 22.39 (t), 14.02 (q, CH_3).

*4.5. Reduction of ketodiesters **2** with $NaBH_3CN$*

To a solution of ketodiester **2a** (0,235 g, 0,89 mmol) in 1mL of MeOH, $NaBH_3CN$ (0,112 g, 1,79 mmol) and glacial acetic acid (0,102 mL, 1,79 mmol) were added. Reaction mixture was stirred for 23 h at room temperature then a saturated solution of $NaHCO_3$ was added until basic pH, methanol was evaporated, H_2O was added and extracted 5 times with ether. Organic phases were dried on anhydrous Na_2SO_4. Evaporation of the solvent afforded a mixture (0.201g) of compounds **3a** (67%, ^{19}F NMR -171,6 ppm), **4a** (22%,^{19}F NMR -175,1 ppm) and **5a** (11%) determined by ^{1}H NMR analysis. The crude reaction mixture was purified by flash chromatography (ethyl acetate-light petroleum, gradient from 4% up to 16%). Before charging the column with the crude reaction mixture, the column was eluted with 3% ethyl acetate in light petroleum with 1ml of glacial acetic acid. A mixture of **3a** and **4a** (0.110 g, 0.42 mmol, 47% yield) was isolated.

***rel*-1,4-Dimethyl (2*R*)-2-fluoro-2-[(1*R*)-1-hydroxyhexyl]-butanedioate 4a**

Spectroscopic data of **4a** were obtained by NMR spectra analysis of mixtures with different composition in **3a** and **4a**, for sake of clarity only the main data which differed from **3a** were reported. ^{1}H NMR (400 MHz, $CDCl_3$): δ 3.85 (s, 3H, OCH_3), 3.1 (m, 2H, H-3), 2.03 (d, 1H,$^{3}J_{HH}$ = 7.4, OH). ^{19}F NMR (376 MHz, $CDCl_3$) δ -175.20 (m). ^{13}C NMR (101 MHz,

$CDCl_3$): δ 170.21 (d, ^2J = 24.2 Hz, C-1), 169.49 (d, ^3J = 2.9 Hz, C-4), 96.73 (d, ^1J = 195.1 Hz, C-2), 74.17 (d, ^2J = 22.2 Hz, CHOH), 38.99 (d, ^2J = 24.1 Hz, C-3).

Reduction of ketodiester **2b** (0.337 g, 1.16 mmol) in 1.2 mL of EtOH with $NaCNBH_3$ (0.146 g, 2.32 mmol) and CH_3COOH (0.133 mL, 2.32 mmol) afforded a mixture (0.263 g, 0.90 mmol) of compounds **3b** (60%, ^{19}F NMR -171,6 ppm) and **4b** (40%,^{19}F NMR -175,1 ppm) and traces of **5b** [39] which didn't need purification.

1,4-Diethyl 2-fluoro-2-(1-hydroxyhexyl)-butanedioates 3b and 4b

Oil. Yield = 78% as a mixture of about 60 and 40% of **3b** and **4b** respectively. ^{1}H NMR (400 MHz, $CDCl_3$): δ 4.40 – 4.25 (m, 2H, OCH_2), 4.16 (q, 2H, $^3J_{HH}$ = 7.1 Hz, OCH_2), 3.86 – 3.65 (m, 1H, C*H*OH), 3.27 – 3.02 (m, 1.4H, H-3), 2.90 (dd, 0.6H, $^2J_{HH}$ = 16.5, $^3J_{HF}$ = 10.1 Hz, H-3), 2.08 (dd, 0.6H, $^3J_{HH}$ = 9.2, $^4J_{HF}$ = 1.7 Hz, OH), 2.06 (dd, 0.4H, $^3J_{HH}$ = 8.8, $^4J_{HF}$ = 1.0 Hz, OH), 1.69 – 1.49 (m, 2H), 1.38 – 1.24 (m, 6H), 1.35 (t, 3H, $^3J_{HH}$ = 7.1 Hz, CH_3), 1.25 (t, 3H, $^3J_{HH}$ = 7.1 Hz, CH_3), 0.89 (t, 3H, $^3J_{HH}$ = 6.8 Hz, CH_3). ^{19}F NMR (376 MHz, $CDCl_3$) δ -171.44 – -171.62 (m, 0.6F, **3b**), -175.11 (m, 0.4F, **4b**). ^{13}C NMR (101 MHz, $CDCl_3$) δ 169.91 (d, ^2J = 24.4 Hz, C-1), 168.81 (s, C-4), 96.56 (d, ^1J = 194.5 Hz, C-2, **4b**), 96.31 (d, ^1J = 194.5 Hz, C-2, **3b**), 74.52 (d, ^2J = 24.4 Hz, CHOH, **3b**), 74.18 (d, ^2J = 22.1 Hz, CHOH, **4b**), 62.25 (s, OCH_2), 61.32 (s, OCH_2), 39.19 (d, ^2J = 24.2 Hz, C-3, **4b**), 39.06 (d, ^2J = 23.1 Hz, C-3, **3b**), 31.66 (s, C-2', **3b**), 31.61 (s, C-2', **4b**), 31.10 (d, ^4J = 2.1 Hz, C-3', **3b**), 31.02 (d, ^4J = 3.5 Hz, C-3', **4b**), 25.59 (s, **4b**), 25.56 (s, **3b**), 22.65 (s), 14.26 (s, CH_3), 14.22 (s, CH_3), 14.13 (s, CH_3). IR (KBr, cm^{-1}): 3495 (OH),1743 (COO). HRMS (ESI) m/z: calcd for $C_{14}H_{25}FO_5Na^+$ $[M+Na]^+$ 315.1578, found 315.1578.

*4.6. General procedure for lactonisation of fluorinated hydroxydiesters **3** and **4***

To the mixuture of **3** and **4** (0.86 mmol) dissolved in 10 mL of CH_2Cl_2, TFA (0.066 mL, 0.86 mmol) was added, the reaction mixture was stirred for 2h. The solvent was evaporated and traces of TFA were removed by coevaporation with diethyl ether (three times).

Lactonisation of **3a** (0.035 g, 0.13 mmol) afforded lactone **6a** (0.027 g, 0.12 mmol) in 92%yield. Lactonisation of the mixture of **3a** and **4a** (0.098 g, 0.37 mmol, 80 and 20% respectively), afforded a mixture of lactones **6a** and **7a** (0.094 g, 83 and 17% respectively) which was purified by flash chromatography (ethyl acetate-light petroleum, gradient from 4% up to 10%). Before charging the column with the crude reaction mixture, the column was eluted with 3% ethyl acetate in light petroleum with 1ml of glacial acetic acid to avoid decomposition of the lactones. Pure lactones **6a** (0.059 g, 0.25 mmol, 67% yield) and **7a** (0.010 g, 0.04 mmol, 11% yield) were isolated.

Lactonisation of the mixture of **3b** and **4b** (0.252 g, 0.86 mmol, 65 and 35% respectively), afforded a mixture of lactones **6b** and **7b** (0.225 g, 63 and 37% respectively) which after purification by flash chromatography gave pure lactones **6b** (0.092 g, 0.37 mmol, 43% yield), **7b** (0.041 g, 0.17 mmol, 19% yield) and a mixture of **6b** and **7b** (0.032 g, 13% yield).

***rel*-(2*R*,3*S*)-Methyl 3-fluoro-5-oxo-2-pentyltetrahydrofuran-3-carboxylate 6a**

Oil. Yield = 92%. ^{1}H NMR (400 MHz, $CDCl_3$): δ 4.63 (ddd, 1H, $^3J_{HF}$ = 22.2, $^3J_{HH}$ = 8.9, $^3J_{HH}$ = 4.8 Hz, H-2), 3.88 (s, 3H, OCH_3), 3.36 (dd, 1H, $^3J_{HF}$ = 26.6, $^2J_{HH}$ = 18.4 Hz, H-4), 2.93 (dd, 1H, $^3J_{HF}$ = 21.4, $^2J_{HH}$ = 18.4 Hz, H-4), 1.58 – 1.46 (m, 2H), 1.43 – 1.23 (m, 6H), 0.89 (t, 3H, $^3J_{HH}$ = 6.9 Hz, CH_3). ^{19}F NMR (376 MHz, $CDCl_3$) δ -152.75 (dt, J = 26.6, 21.8 Hz). ^{13}C NMR (101 MHz, $CDCl_3$) δ 171.53 (d, ^3J = 2.4 Hz, C-5), 166.99 (d, ^2J = 27.3 Hz, COO), 98.01 (d, ^1J = 197.0 Hz, C-3), 85.47 (d, ^2J = 28.7 Hz, H-2), 53.53 (s, OCH_3), 38.29 (d, ^2J = 23.5 Hz, C-4), 31.31 (s), 30.93 (d, ^3J = 4.9 Hz, C-1'), 25.14 (s), 22.50 (s), 14.04 (s, CH_3). IR (film, cm^{-1}): 1799, 1753. HRMS (ESI) m/z: calcd for $C_{11}H_{17}FO_4Na^+$ $[M+Na]^+$ 255.1003, found 255.1001.

***rel*-(2*R*,3*R*)-Methyl 3-fluoro-5-oxo-2-pentyltetrahydrofuran-3-carboxylate 7a**

Oil. Yield = 11%. ^{1}H NMR (400 MHz, $CDCl_3$): δ 4.70 (ddd, 1H, $^3J_{HF}$ = 22.2, $^3J_{HH}$ = 8.7, $^3J_{HH}$ = 5.1 Hz, H-2), 3.89 (s, 3H, OCH_3), 3.25 (dd, 1H, $^3J_{HF}$ = 34.8, $^2J_{HH}$ = 18.3 Hz, H-4), 2.96 (dd, 1H, $^3J_{HF}$ = 20.6, $^2J_{HH}$ = 18.2 Hz, H-4), 1.93 – 1.81 (m, 1H), 1.70 (m, 1H), 1.54 – 1.22 (m, 6H), 0.89 (t, 3H, $^3J_{HH}$ = 7.1 Hz, CH_3). ^{19}F NMR (376 MHz, $CDCl_3$) δ -173.66 (dt, J = 34.9, 21.3 Hz). ^{13}C NMR (101 MHz, $CDCl_3$) δ 171.51 (d, ^3J = 0.5 Hz, C-5), 167.95 (d, ^2J = 26.4 Hz, COO), 96.49 (d, ^1J = 203.3 Hz, C-3), 84.90 (d, ^2J = 23.0 Hz, C-2), 53.81 (s, OCH_3), 40.78 (d, ^2J = 26.2 Hz, C-4), 31.51 (s), 28.00 (d, ^3J = 8.0 Hz, C-1'), 25.05 (s), 22.48 (s), 14.04 (s, CH_3). IR (film, cm^{-1}): 1797, 1747. HRMS (ESI) m/z: calcd for $C_{11}H_{17}FO_4Na^+$ $[M+Na]^+$ 255.1003, found 255.1003.

***rel*-(2*R*,3*S*)-Ethyl 3-fluoro-5-oxo-2-pentyltetrahydrofuran-3-carboxylate 6b**

Oil. Yield = 43%. ^{1}H NMR (400 MHz, $CDCl_3$): δ 4.63 (m, 1H, $^3J_{HF}$ = 22.2 Hz, H-2), 4.34 (q, 2H, $^3J_{HH}$ = 7.1 Hz, OCH_2), 3.36 (dd, 1H, $^3J_{HF}$ = 26.5, $^2J_{HH}$ =18.4 Hz, H-4 *trans* to F), 2.93 (dd, 1H, $^3J_{HF}$ = 21.5, $^2J_{HH}$ =18.4 Hz, H-4 *cis* to F), 1.60 – 1.47 (m, 3H), 1.36 (t, 3H, $^3J_{HH}$ = 7.1 Hz, CH_3), 1.33 (m, 5H), 0.89 (t, 3H, $^3J_{HH}$ = 7.0 Hz, CH_3). ^{19}F NMR (376 MHz, $CDCl_3$) δ -152.59 (dt, J = 26.5, 21.8 Hz). ^{13}C NMR (101 MHz, $CDCl_3$) δ 171.64 (d, ^3J = 2.7 Hz, C-5), 166.51 (d, ^2J = 27.1 Hz, COO), 97.90 (d, ^1J = 196.8 Hz, C-3), 85.50 (d, ^2J = 28.8 Hz, C-2), 63.11 (s, OCH_2), 38.31 (d, ^2J = 23.5 Hz, C-4), 31.31 (s), 30.91 (d, ^3J = 4.9 Hz, C-1'), 25.13 (s), 22.49 (s), 14.22 (s, CH_3), 14.05 (s, CH_3). IR (KBr, cm^{-1}): 1799, 1760, 1747. HRMS (ESI) m/z: calcd for $C_{12}H_{19}FO_4Na^+$ $[M+Na]^+$ 269.1159, found 269.1159.

***rel*-(2*R*,3*R*)-Ethyl 3-fluoro-5-oxo-2-pentyltetrahydrofuran-3-carboxylate 7b**

Oil. Yield = 19%. ^{1}H NMR (400 MHz, $CDCl_3$): δ 4.70 (ddd, 1H, $^3J_{HF}$ = 22.1, $^3J_{HH}$ = 8.5, $^3J_{HH}$ = 5.4 Hz, H-2), 4.40 – 4.27 (m, 2H, OCH_2), 3.25 (dd, 1H, $^3J_{HF}$ = 34.8, $^2J_{HH}$ = 18.3 Hz, H-4 *cis* to F), 2.96 (dd, 1H, $^3J_{HF}$ = 20.6, $^3J_{HH}$ = 18.3 Hz, H-4 *trans* to F), 1.87 (m, 1H), 1.71 (m, 1H), 1.53 – 1.09 (m, 6H), 1.35 (t, $^3J_{HH}$ = 7.1 Hz, 3H, CH_3), 0.89 (t, 3H, $^3J_{HH}$ = 6.9 Hz, CH_3). ^{19}F NMR (376 MHz, $CDCl_3$) δ -173.71 (dt, J = 34.7, 21.3 Hz). ^{13}C NMR (101 MHz, $CDCl_3$) δ 171.64 (d, ^3J = 0.7 Hz, C-5), 167.47 (d, ^2J = 26.4 Hz, COO), 96.43 (d, ^1J = 203.3 Hz, C-3), 84.93 (d, ^2J = 23.0 Hz, C-2), 63.30 (s, OCH_2), 40.78 (d, ^2J = 26.2 Hz, C-4), 31.52 (s), 28.02 (d, ^3J = 8.0 Hz, C-1'), 25.01 (s), 22.49 (s), 14.20 (s, CH_3), 14.04 (s, CH_3). IR (KBr, cm^{-1}): 1789, 1764, 1743. HRMS (ESI) m/z: calcd for $C_{12}H_{19}FO_4Na^+$ $[M+Na]^+$ 269.1159, found 269.1160.

*4.7. Synthesis of lactones **10, 11** and **12***

Ketodiester **9** (0.58 g, 2.8 mmol) was reduced with $NaBH_3CN$ following the procedure described above, the crude reaction mixture was treated with TFA and the NMR analysis of the crude indicated the presence of lactones **10, 11** and **12** in 2:1:2.6 ratio respectively. Purification by flash chromatography (gradient from 10% ethyl acetate, 90% light petroleum + 0.5% acetic acid up to 20% ethyl acetate, 80% light petroleum + 0.5% acetic acid) afforded 0.166 g of an inseparable mixture of lactones **10** and **12** in 2:3 ratio respectively and 0.050 g (0.28 mmol, 10% yield) of lactone **11**.

***rel*-(2*R*,3*S*)-Methyl 3-fluoro-2-methyl-5-oxotetrahydrofuran-3-carboxylate 10 and Methyl 2-methyl-5-oxo-2,5-dihydrofuran-3-carboxylate 12**

For sake of clarity NMR data are given separately. Compound **10**: ^{1}H NMR (400 MHz, $CDCl_3$) δ 4.82 (dq, 1H, $^3J_{HF}$ = 22.1, $^3J_{HH}$ = 6.9 Hz, H-2), 3.89 (s, 3H, OCH_3), 3.40 (dd, 1H, $^3J_{HF}$ = 28.4, $^2J_{HH}$ = 18.5 Hz, H-4), 2.93 (ddd, 1H, $^3J_{HF}$= 21.5, $^2J_{HH}$ =18.5, $^4J_{HH}$ = 0.5 Hz, H-4), 1.33 (d, 3H, $^3J_{HH}$ = 6.8 Hz). ^{19}F NMR (376 MHz, CDCl3) δ -153.18 (dt, J = 28.4, 21.7 Hz). ^{13}C NMR (101 MHz, CDCl3) δ 171.27 (d, ^3J = 2.2 Hz, C-5), 166.60 (d, ^2J = 27.2 Hz, COO), 98.16 (d, ^1J = 196.5 Hz, C-3), 81.61 (d, ^2J = 29.7 Hz, C-2), 53.39 (s), 37.58 (d, ^{2}J = 23.8 Hz, C-4), 16.46 (d, ^3J = 6.1 Hz, CH_3). HRMS (ESI) m/z: calcd for $C_7H_9FO_4Na^+$ $[M+Na]^+$ 199.0377, found 199.0382 .

Compound **12**: ^{1}H NMR (400 MHz, $CDCl_3$) δ 6.66 (d, 1H, ^4J = 1.9 Hz,

H-4), 5.28 (qd, 1H, $^{3}J = 6.7$, $^{4}J = 1.9$ Hz, H-2), 3.90 (s, 3H, OCH_3), 1.59 (d, 3H, $^{3}J = 6.7$ Hz, CH_3). ^{13}C NMR (101 MHz, $CDCl_3$) δ 170.69 (s, C-5), 161.30 (s, COO), 158.29 (s, C-3), 126.57 (d, C-4), 78.95 (d, C-2), 52.79 (q, OCH_3), 18.70 (q, CH_3). HRMS (ESI) m/z: calcd for $C_7H_8O_4Na^+$ $[M+Na]^+$ 179.0315, found 179.0311.

***rel*-(2*R*,3*R*)-Methyl 3-fluoro-2-methyl-5-oxotetrahydrofuran-3-carboxylate 11**

Oil. Yield = 10%. ^{1}H NMR (400 MHz, $CDCl_3$) δ 4.83 (dq, 1H, $^{3}J_{HF} = 21.7$, $^{3}J_{HH} = 6.5$ Hz, H-2), 3.89 (s, 3H, OCH_3), 3.28 (dd, 1H, $^{3}J_{HF} = 35.0$, $^{2}J_{HH} = 18.3$ Hz, H-4), 2.97 (dd, 1H, $^{3}J_{HF} = 20.4$, $^{2}J_{HH} = 18.3$ Hz, H-4), 1.47 (dd, 3H, $^{3}J_{HH} = 6.6$, $^{4}J_{HF} = 2.4$ Hz, CH_3). ^{19}F NMR (376 MHz, $CDCl_3$) δ -173.80 (dtq, $J = 34.9, 22.4, 2.4$ Hz). ^{13}C NMR (101 MHz, CDCl3) δ 171.39 (s, C-5), 167.29 (d, $^{2}J = 26.4$ Hz, COO), 96.54 (d, $^{1}J = 202.5$ Hz, C-3), 80.78 (d, $^{2}J = 23.5$ Hz, C-2), 53.67 (s, OCH_3), 40.27 (d, $^{2}J = 26.0$ Hz, C-4), 12.86 (d, $^{3}J = 10.3$ Hz, CH_3). HRMS (ESI) m/z: calcd for $C_7H_9FO_4Na^+$ $[M+Na]^+$ 199.0377, found 199.0376.

4.8. Computational details

We wrote a Python script in a Jupiter notebook (see SI) for conformer generation by RDKit, version 2019.03.2 [47]. The molecules were loaded as SMILES, then added with hydrogens and embedded generating 100 conformers [48], successively minimized employing the MMFF force field. The Cremer puckering parameters were calculated in the same notebook according to ref. [63].

The DFT protocol used for the calculation of ^{19}F NMR shieldings is similar to that outlined in references [64,65]. The equilibrium structure of the four selected lowest energy conformers of methyl esters (2*R*, 3*S*)-**6a** and (2*R*,3*R*)-**7a**, ^{3}E and E_3 for each, and the analogous four lowest energy conformers of ethyl esters (2*R*,3*S*)-**6b** and (2*R*,3*R*)-**7b**, were optimized at the density functional theory (DFT), within the generalized gradient approximation (GGA), using the BLYP functional [66,67] and a triple-ζ twice-polarized basis of Slater-type orbitals (TZ2P). Scalar relativistic effects were included within the zero-order regular approximation (ZORA). A subsequent vibrational frequency analysis yielded all positive frequencies, confirming that the stationary points were true minima of the potential energy surface.

The calculation of ^{19}F NMR chemical shifts has been carried out using two-component relativistic DFT based on the ZORA Hamiltonian and gauge-including basis functions (GIAOs) implemented in the ADF program [68,69], and the routines for the calculation of NMR properties [70,71]. Computed NMR shielding can be written as a sum of two contributions:

$$\sigma = \sigma_d + \sigma_{p+SO} \quad (2)$$

where the different symbols stand for the diamagnetic (σ_d), and paramagnetic plus spin-orbit (σ_{p+SO}) terms. Computed chemical shifts are referenced to $CFCl_3$ (σ_{ref}=120.96 ppm with the given combination of xc DFT functional and basis set). For a better comparison with the experimental values, we have adopted the correlation between calculated and experimental ^{19}F chemical shifts of Saielli et al. [64], namely:

$$\delta_{calc} = a + b\delta_{exp} \quad (3)$$

with a = -17 ppm and b = 1.15.

The localized orbital-based NMR shielding analysis is carried out based on scalar relativistic natural bonding orbitals (NBOs), and natural localized molecular orbitals (NLMOs) [72-74] obtained with the NBO 6.0 program [75], and included in the ADF distribution. The plots of p+SO contributions were performed using the open source software Matplotlib [76] version 3.3.4 [77]

Declaration of Competing Interest

The authors declare that they have no known competing financial interests or personal relationships that could have appeared to influence the work reported in this paper.

Acknowledgments

We are grateful to University of Trieste (FRA 2018 and FRA 2020) for financial support.

References

[1] M. Inoue, Y. Sumii, N. Shibata, Contribution of Organofluorine Compounds to Pharmaceuticals, ACS Omega 5 (2020) 10633–10640, https://doi.org/10.1021/acsomega.0c00830.
[2] J. Han, A.M. Remete, L.S. Dobson, L. Kiss, K. Izawa, H. Moriwaki, V.A. Soloshonok, D. O'Hagan, Next generation organofluorine containing blockbuster drugs, J. Fluorine Chem. 239 (2020), 109639, https://doi.org/10.1016/j.jfluchem.2020.109639.
[3] P.W.A. Howe, Recent developments in the use of fluorine NMR in synthesis and characterization, Prog. Nucl. Magn. Reson. Spectrosc. 1 (2020) 118–119, https://doi.org/10.1016/j.pnmrs.2020.02.002.
[4] B.G.de la Torre, F. Albericio, The Pharmaceutical Industry in 2019. An Analysis of FDA Drug Approvals from the Perspective of Molecules, Molecules 25 (2020) 745, https://doi.org/10.3390/molecules25030745.
[5] R.D. Chambers, Fluorine in Organic Chemistry, Blackwell Publishing Ltd, Oxford, 2004.
[6] E.P. Gillis, K.J. Eastman, M.D. Hill, D.J. Donnelly, N.A. Meanwell, Applications of Fluorine in Medicinal Chemistry, J. Med. Chem. 58 (2015) 8315–8359, https://doi.org/10.1021/acs.jmedchem.5b00258.
[7] B. Hong, T. Luo, X. Lei, Late-Stage Diversification of Natural Products, ACS Cent. Sci. 6 (2020) 622–635, https://doi.org/10.1021/acscentsci.9b00916.
[8] P. Ertl, E. Altmann, J.M. McKenna, The Most Common Functional Groups in Bioactive Molecules and How Their Popularity Has Evolved over Time, J. Med. Chem. 63 (2020) 8408–8418, https://doi.org/10.1021/acs.jmedchem.0c00754.
[9] P.A. Champagne, J. Desroches, J.-D. Hamel, M. Vandamme, J.-Fr. Paquin, Monofluorination of Organic Compounds: 10 Years of Innovation, Chem. Rev. 115 (2015) 9073–9174, https://doi.org/10.1021/cr500706a.
[10] R. Bandichhor, B. Nosse, O. Reiser, Paraconic Acids—The Natural Products from Lichen Symbiont, in: J. Mulzer (Ed.), Natural Product Synthesis I: Targets, Methods, Concepts, Springer Berlin Heidelberg, Berlin, Heidelberg, 2005, pp. 43–72, https://doi.org/10.1007/b96881.
[11] S. Haleema, P.V. Sasi, I. Ibnusaud, P.L. Polavarapu, H.B. Kagan, Enantiomerically pure com-pounds related to chiral hydroxy acids derived from renewable resources, RSC Adv 2 (2012) 9257–9285, https://doi.org/10.1039/C2RA21205F.
[12] C. Forzato, P. Nitti, G. Pitacco, E. Valentin, Recent aspects of the synthesis of enantiopure 5-oxo-tetrahydro-3-furancarboxylic acids, O. A. Attanasi, D. Spinelli editors, in: Targets in heterocy-clic systems, Vol.3, The Italian Society of Chemistry, Rome, 1999, pp. 93–115.
[13] K. Chakrabarty, I. Defrenza, N. Denora, S. Drioli, C. Forzato, M. Franco, G. Lentini, P. Nitti, G. Pitacco, Enzymatic Resolution of α-Methyleneparaconic Acids and Evaluation of their Biological Activity, Chirality 27 (2015) 239–246, https://doi.org/10.1002/chir.22419, and references cited therein.
[14] V. Lehner, H.M.L. Davies, O. Reiser, Rh(II)-Catalyzed Cyclopropanation of Furans and Its Application to the Total Synthesis of Natural Product Derivatives, Org. Lett. 19 (2017) 4722–4725, https://doi.org/10.1021/acs.orglett.7b02009.
[15] R. Gérardy, M. Winter, C.R. Horn, A. Vizza, K. Van Hecke, J.-C.M. Monbaliu, Continuous-Flow Preparation of γ-Butyrolactone Scaffolds from Renewable Fumaric and Itaconic Acids under Photosensitized Conditions, Org. Process Res. Dev. 21 (2017) 2012–2017, https://doi.org/10.1021/acs.oprd.7b00314.
[16] J.L. Nallasivam, R.A. Fernandes, A protecting-group-free synthesis of (+)-nephrosteranic, (+)-protolichesterinic, (+)-nephrosterinic, (+)-phaseolinic, (+)-rocellaric acids and (+)-methylenolactocin, Org. Biomol. Chem. 15 (2017) 708–716, https://doi.org/10.1039/C6OB02398C.
[17] S. Phae-nok, D. Soorukram, C. Kuhakarn, V. Reutrakul, M. Pohmakotr, Silver-Mediated De-carboxylative Fluorination of Paraconic Acids: A Direct Entry to β-Fluorinated γ-Butyrolactones, Eur. J. Org. Chem. (2015) 2879–2888, https://doi.org/10.1002/ejoc.201500023, 2015.
[18] O.V. Turova, E.V. Starodubtseva, M.G. Vinogradov, V.A. Ferapontov, M. I. Struchkova, A concise synthesis of highly enantiomerically enriched 2-alkyl-paraconic acid esters via ruthenium-catalyzed asymmetric hydrogenation of acylsuccinates, Tetrahedron: Asymm 20 (2009) 2121–2124, https://doi.org/10.1016/j.tetasy.2009.09.006.
[19] A. Comini, C. Forzato, P. Nitti, G. Pitacco, E. Valentin, Chemoenzymatic synthesis of enantioenriched 5-oxo-tetrahydro-3-furancarboxylic acid derivatives, Tetrahedron: Asymm 15 (2004) 617–625, https://doi.org/10.1016/j.tetasy.2004.01.001.
[20] F. Berti, F. Felluga, C. Forzato, G. Furlan, P. Nitti, G. Pitacco, E. Valentin, Chemoenzymatic synthesis of diastereomeric ethyl γ-benzyl paraconates and

determination of the absolute configura-tions of their acids, Tetrahedron: Asymm 17 (2006) 2344–2353, https://doi.org/10.1016/j.tetasy.2006.08.013.
[21] C. Forzato, G. Furlan, P. Nitti, G. Pitacco, E. Valentin, E. Zangrando, P. Buzzini, M. Goretti, B. Turchetti, Chemoenzymatic and yeast-catalysed synthesis of diastereomeric ethyl γ-phenyl and γ-(n-pyridyl)paraconates, Tetrahedron: Asymm 19 (2008) 2026–2036, https://doi.org/10.1016/j.tetasy.2008.08.011.
[22] A. Bertogg, L. Hintermann, D.P. Huber, M. Perseghini, M. Sanna, A. Togni, Substrate Range of the Titanium TADDOLate Catalyzed Asymmetric Fluorination of Activated Carbonyl Com-pounds, Helv. Chim. Acta 95 (2012) 353–403, https://doi.org/10.1002/hlca.201100375.
[23] J.-C. Xiao, J.M. Shreeve, Microwave-assisted rapid electrophilic fluorination of 1,3-dicarbonyl derivatives with Selectfluor®, J. Fluorine Chem. 126 (2005) 473–476, https://doi.org/10.1016/j.jfluchem.2004.10.043.
[24] T. Punirun, D. Soorukram, C. Kuhakarn, V. Reutrakul, M. Pohmakotr, Stereoselective Synthe-sis of 1-Fluoro-exo,exo-2,6-diaryl-3,7-dioxabicyclo[3.3.0] octanes: Synthesis of (±)-1-Fluoromembrine, J. Org. Chem. 80 (2015) 7946–7960, https://doi.org/10.1021/acs.joc.5b00970.
[25] S. Drioli, F. Felluga, C. Forzato, P. Nitti, G. Pitacco, A facile route to (+)- and (–)-trans-tetrahydro-5-oxo-2-pentylfuran-3-carboxylic acid, precursors of (+)- and (–)-methylenolactocin, Chem. Commun. (1996) 1289–1290, https://doi.org/10.1039/CC9960001289.
[26] M.B.M. De Azevedo, M.M. Murta, A.E. Greene, Novel, enantioselective lactone construction. First synthesis of methylenolactocin, antitumor antibiotic from Penicillium sp, J. Org. Chem. 57 (1992) 4567–4569, https://doi.org/10.1021/jo00043a003.
[27] M. Tredwell, J.A.R. Luft, M. Schuler, K. Tenza, K.N. Houk, V. Gouverneur, Fluorine-Directed Diastereoselective Iodocyclizations, Angew. Chem. Int. Ed. 47 (2008) 357–360, https://doi.org/10.1002/anie.200703465.
[28] W.R. Dolbier Jr., Guide to Fluorine NMR for Organic Chemists, Wiley Online Books, 2016, https://doi.org/10.1002/9781118831106.
[29] W.A. Thomas, Unravelling molecular structure and conformation—the modern role of coupling constants, Prog. Nucl. Magn. Reson. Spectrosc. 30 (1997) 183–207, https://doi.org/10.1016/S0079-6565(96)01033-3.
[30] C. Thibaudeau, J. Plavec, J. Chattopadhyaya, A New Generalized Karplus-Type Equation Relating Vicinal Proton-Fluorine Coupling Constants to H−C−C−F Torsion Angles, J. Org. Chem. 63 (1998) 4967–4984, https://doi.org/10.1021/jo980144k.
[31] C. Jaime, R.M. Ortuno, J. Font, Di- and trisubstituted γ-lactones. Conformational study by molecular mechanics calculations and coupling constant analysis, J. Org. Chem. 51 (1986) 3946–3951, https://doi.org/10.1021/jo00371a006.
[32] C.A. Stortz, M.S. Maier, Configurational assignments of diastereomeric γ-lactones using vicinal H–H NMR coupling constants and molecular modelling, J. Chem. Soc., Perkin Trans. 2 (2000) 1832–1836, https://doi.org/10.1039/B003862H.
[33] C.I. Viturro, M.S. Maier, C.A. Stortz, J.R. de la Fuente, Antifungal diastereomeric furanones from Mutisia friesiana: structural determination and conformational analysis, Tetrahedron: Asymm 12 (2001) 991–998, https://doi.org/10.1016/S0957-4166(01)00163-X.
[34] L.E. Combettes, P. Clausen-Thue, M.A. King, B. Odell, A.L. Thompson, V. Gouverneur, D.W. Claridge, Conformational Analysis of Fluorinated Pyrrolidines Using ^{19}F–1H Scalar Couplings and Heteronuclear NOEs, Chem. Eur. J. 18 (2012) 13133–13141, https://doi.org/10.1002/chem.201201577.
[35] T.M. Patrick, The free Radical Addition of aldehydes to Unsaturated Polycarboxylic Esters, J. Org. Chem. 17 (1952) 1009–1016, https://doi.org/10.1021/jo50007a016.
[36] V. Chudasama, R.J. Fitzmaurice, S. Caddick, Hydroacylation of α,β-unsaturated esters via aerobic C–H activation, Nat. Chem. 2 (2010) 592–596, https://doi.org/10.1038/nchem.685.
[37] D. O'Hagan, Understanding organofluorine chemistry. An introduction to the C–F bond, Chem. Soc. Rev. 37 (2008) 308–319, https://doi.org/10.1039/B711844A.
[38] M. Kato, M. Kageyama, R. Tanaka, K. Kuwahara, A. Yoshikoshi, Synthetic study of (+-)-canadensolide and related dilactones. Double lactonization of unsaturated dicarboxylic acids via acyl hypoiodite intermediates, J. Org. Chem. 40 (1975) 1932–1941, https://doi.org/10.1021/jo00901a014.
[39] N. Selvakumar, P. Kalyan Kumar, K. Chandra Shekar Reddy, B. Chandra Chary, Synthesis of substituted butenolides by the ring closing metathesis of two electron deficient olefins: a general route to the natural products of paraconic acids class, Tetrahedron Lett 48 (2007) 2021–2024, https://doi.org/10.1016/j.tetlet.2007.01.053.
[40] A. Macchioni, A. Magistrato, I. Orabona, F. Ruffo, U. Rothlisberger, C. Zuccaccia, Direct observation of an equilibrium between two anion-cation orientations in olefin Pt(II) complex ion pairs by HOESY NMR spectroscopy, New J. Chem. 27 (2003) 455–458, https://doi.org/10.1039/B212088G.
[41] A. Macchioni, Elucidation of the Solution Structures of Transition Metal Complex Ion Pairs by NOE NMR Experiments, Eur. J. Inorg. Chem. (2003) 195–205, https://doi.org/10.1002/ejic.200390026, 2003and references therein.
[42] S. Macura, R.R. Ernst, Elucidation of cross relaxation in liquids by two-dimensional N.M.R. spectroscopy, Mol. Phys. 41 (1980) 95–117, https://doi.org/10.1080/00268978000102601.
[43] J. Tropp, Dipolar relaxation and nuclear Overhauser effects in nonrigid molecules: The effect of fluctuating internuclear distances, J. Chem. Phys. 72 (1980) 6035–6043, https://doi.org/10.1063/1.439059.
[44] P.F. Yip, D.A. Case, J.C. Hoch, F.M. Poulsen, C. Redfield, Computational As-pect of the Study of Biological Macromolecules by Nuclear Magnetic Resonance Spectroscopy, Plenum Press, New York, 1991, pp. 317–330, https://doi.org/10.1007/978-1-4757-9794-7.
[45] A. Kolmer, L.J. Edwards, I. Kuprov, C.M. Thiele, Conformational analysis of small organic molecules using NOE and RDC data: A discussion of strychnine and α-methylene-γ-butyrolactone, J. Magn. Reson. 261 (2015) 101–109, https://doi.org/10.1016/j.jmr.2015.10.007.
[46] C.A. Stortz, A.M. Sarotti, Exhaustive exploration of the conformational landscape of mono- and disubstituted five-membered rings by DFT and MP2 calculations, RSC Adv 9 (2019) 24134–24145, https://doi.org/10.1039/C9RA03524A.
[47] https://www.rdkit.org DOI: 10.5281/zenodo.591637.
[48] J.-P. Ebejer, G.M. Morris, C.M. Deane, Freely Available Conformer Generation Methods: How Good Are They ? J. Chem. Inf. Model. 52 (2012) 1146–1158, https://doi.org/10.1021/ci2004658.
[49] I.Y. Kanal, J.A. Keith, G.R. Hutchison, A sobering assessment of small-molecule force field methods for low energy conformer predictions, Int. J. Quantum Chem. 118 (2018) e25512, https://doi.org/10.1002/qua.25512.
[50] D. Marchesan, S. Coriani, C. Forzato, P. Nitti, G. Pitacco, K. Ruud, Optical Rotation Calculation of a Highly Flexible Molecule: The Case of Paraconic Acid, J. Phys. Chem. A 109 (2005) 1449–1453, https://doi.org/10.1021/jp047108b.
[51] J.P. Foster, F. Weinhold, Natural hybrid orbitals, J. Am. Chem. Soc. 102 (1980) 7211–7218, https://doi.org/10.1021/ja00544a007.
[52] A.E. Reed, F. Weinhold, Natural localized molecular orbitals, J. Chem. Phys. 83 (1985) 1736–1740, https://doi.org/10.1063/1.449360.
[53] F. Weinhold, Encyclopedia of Computational Chemistry, P. von Rague' Schleyer, Wiley, Chichester, 1998, pp. 1792–1811.
[54] S. Moncho, J. Autschbach, Molecular orbital analysis of the inverse halogen dependence of nuclear magnetic shielding in LaX3, X = F, Cl, Br, I, Magn. Reson. Chem. 48 (2010) S76–S85, https://doi.org/10.1002/mrc.2632.
[55] W. Adcock, J.E. Peralta, R.H. Contreras, Computation and analysis of ^{19}F substituent chemical shifts of some bridgehead-substituted polycyclic alkyl fluorides, Magn. Reson. Chem. 41 (2003) 503–508, https://doi.org/10.1002/mrc.1202.
[56] C. Kasireddy, J.G. Bann, K.R. Mitchell-Koch, Demystifying fluorine chemical shifts: electronic structure calculations address origins of seemingly anomalous^{19}F-NMR spectra of fluorohistidine isomers and analogues, Phys. Chem. Chem. Phys. 17 (2015) 30606–30612, https://doi.org/10.1039/C5CP05502D.
[57] A. Ouchi, C. Liu, M. Kaneda, T. Hyugano, Photochemical C–C Bond Formation between Alcohols and Olefins by an Environmentally Benign Radical Reaction, Eur. J. Org. Chem. (2013) 3807–3816, https://doi.org/10.1002/ejoc.201300115, 2013.
[58] S. Coriani, A. Baranowska, L. Ferrighi, C. Forzato, D. Marchesan, P. Nitti, G. Pitacco, A. Rizzo, K. Ruud, Solvent effects on the conformational distribution and optical rotation of γ-methyl paraconic acids and esters, Chirality 18 (2006) 357–369, https://doi.org/10.1002/chir.20261.
[59] Y. Zhu, J. Han, J. Wang, N. Shibata, M. Sodeoka, V.A. Soloshonok, J.A.S. Coelho, F. D. Toste, Modern Approaches for Asymmetric Construction of Carbon–Fluorine Quaternary Stereogenic Centers: Synthetic Challenges and Pharmaceutical Needs, Chem. Rev. 118 (7) (2018) 3887–3964.
[60] B. Lix, F.D. Sönnichsen, B.D. Sykes, The Role of Transient Changes in Sample Susceptibility in Causing Apparent Multiple-Quantum Peaks in HOESY Spectra, J. Magn. Reson. A 121 (1996) 83–87, https://doi.org/10.1006/jmra.1996.0141.
[61] M. Loos, C. Gerber, F. Corona, J. Hollender, H. Singer, Accelerated Isotope Fine Structure Calculation Using Pruned Transition Trees, Anal. Chem. 87 (2015) 5738–5744, https://doi.org/10.1021/acs.analchem.5b00941.
[63] D. Cremer, J.A. Pople, General definition of ring puckering coordinates, J. Am. Chem. Soc. 97 (1975) 1354–1358, https://doi.org/10.1021/ja00839a011.
[64] G. Saielli, R. Bini, A. Bagno, Computational^{19}F NMR. 2. Organic compounds, RSC Adv 4 (2014) 41605–41611, https://doi.org/10.1039/C4RA08290G.
[65] G. Saielli, R. Bini, A. Bagno, Computational ^{19}F NMR. 1. General features, Theor. Chem. Acc. 131 (2012) 1140, https://doi.org/10.1007/s00214-012-1140-z.
[66] A.D. Becke, Density-functional exchange-energy approximation with correct asymptotic behavior, Phys. Rev. A 38 (1988) 3098–3100, https://doi.org/10.1103/PhysRevA.38.3098.
[67] C. Lee, W. Yang, R.G. Parr, Development of the Colle-Salvetti correlation-energy formula into a functional of the electron density, Phys. Rev. B 37 (1988) 785–789, https://doi.org/10.1103/PhysRevB.37.785.
[68] G. te Velde, F.M. Bickelhaupt, E.J. Baerends, C. Fonseca Guerra, S.J.A. van Gisbergen, J.G. Snijders, T. Ziegler, Chemistry with ADF, J. Comput. Chem. 22 (2001) 931–967, https://doi.org/10.1002/jcc.1056.
[69] ADF, SCM, Theoretical Chemistry, Vrije Universiteit, Amsterdam, The Netherlands, 2020. http://www.scm.com.
[70] S.K. Wolff, T. Ziegler, E. van Lenthe, E.J. Baerends, Density functional calculations of nuclear magnetic shieldings using the zeroth-order regular approximation (ZORA) for relativistic effects: ZORA nuclear magnetic resonance, J. Chem. Phys. 110 (1999) 7689–7698, https://doi.org/10.1063/1.478680.
[71] J. Autschbach, E. Zurek, Relativistic Density-Functional Computations of the Chemical Shift of 129Xe in Xe@C60, J. Phys. Chem. A 107 (2003) 4967–4972, https://doi.org/10.1021/jp0346559.
[72] J. Autschbach, Analyzing NMR shielding tensors calculated with two-component relativistic methods using spin-free localized molecular orbitals, J. Chem. Phys. 128 (2008), 164112, https://doi.org/10.1063/1.2905235.
[73] J. Autschbach, S. Zheng, Analyzing Pt chemical shifts calculated from relativistic density functional theory using localized orbitals: The role of Pt 5d lone pairs, Magn. Reson. Chem. 46 (2008) S45–S55, https://doi.org/10.1002/mrc.2289.
[74] J. Autschbach, Analyzing molecular properties calculated with two-component relativistic methods using spin-free natural bond orbitals: NMR spin-spin coupling constants, J. Chem. Phys. 127 (2007), 124106, https://doi.org/10.1063/1.2768363.

[75] E.D. Glendening, J.K. Badenhoop, A.E. Reed, J.E. Carpenter, J.A. Bohmann, C. M. Morales, C.R. Landis, F. Weinhold, NBO 6.0, Theoretical Chemistry Institute, University of Wisconsin, Madison, WI, 2013. http://nbo6.chem.wisc.edu/.
[76] J.D. Hunter, Matplotlib: A 2D Graphics Environment, Comp. Sci. Engin. 9 (3) (2007) 90–95, https://doi.org/10.1109/MCSE.2007.55.
[77] T.A. Caswell, M. Droettboom, A. Lee, E.S. de Andrade, J. Hunter, E. Firing, T. Hoffmann, J. Klymak, D. Stansby, N. Varoquaux, J.H. Nielsen, B. Root, R. May, P. Elson, J.K. Seppänen, D. Dale, J.-J. Lee, D. McDougall, A. Straw, P. Hobson, C. Gohlke, T.S. Yu, E. Ma, A.F. Vincent, hannah, S. Silvester, C. Moad, N. Kniazev, E. Ernest, P. Ivanov, matplotlib/matplotlib: REL: v3.3.4, Zenodo, 2021. https://doi.org/10.5281/zenodo.4475376.